

# Sequential changepoint detection for label shift in classification

Ciaran Evans\* and Max G’Sell†

Department of Statistics and Data Science, Carnegie Mellon University

November 22, 2021

## Abstract

Classifier predictions often rely on the assumption that new observations come from the same distribution as training data. When the underlying distribution changes, so does the optimal classifier rule, and predictions may no longer be valid. We consider the problem of detecting a change to the overall fraction of positive cases, known as label shift, in sequentially-observed binary classification data. We reduce this problem to the problem of detecting a change in the one-dimensional classifier scores, which allows us to develop simple nonparametric sequential changepoint detection procedures. Our procedures leverage classifier training data to estimate the detection statistic, and converge to their parametric counterparts in the size of the training data. In simulations, we show that our method compares favorably to other detection procedures in the label shift setting.

## 1 Problem setup and background

We consider the problem of detecting changes in the distribution of sequentially-observed classification data, which is important for making valid predictions in dynamic situations. Binary classification problems typically involve observations of the form  $(X_i, Y_i) \in \mathbb{R}^d \times \{0, 1\}$ . In a supervised setting, training observations  $(X'_1, Y'_1), \dots, (X'_{n_{train}}, Y'_{n_{train}})$  are used to construct a classifier  $\mathcal{A}(\cdot)$ , which aims to predict future labels  $Y_i$  using  $\mathcal{A}(X_i)$ . However, if the training and evaluation data distributions are different,  $(X_i, Y_i) \neq (X'_i, Y'_i)$ , performance of the classifier predictions  $\mathcal{A}(X_i)$  may change. Furthermore, a change in the data distribution may reflect an underlying change of interest in the application domain. This general problem of mismatched distributions has been studied extensively in the literature, as we review in Section 1.4.

We consider the setting where new observations  $X_1, X_2, X_3, \dots$  of classifier features arrive sequentially. Our classifier  $\mathcal{A}(\cdot)$  is fixed, and with each new observation  $X_i$  we make a prediction  $\mathcal{A}(X_i)$  – the true labels  $Y_1, Y_2, Y_3, \dots$  remain unobserved. At some time  $\nu \geq 0$  in this sequence, the distribution of  $(X_i, Y_i)$  changes. Since a change means our classifier predictions  $\mathcal{A}(X_i)$  may no longer be valid, our aim is to detect a change in the distribution of  $(X_i, Y_i)$  as quickly as possible, using the observed sequence  $X_i$ . This manuscript focuses on a particular class of distributional changes call *label shift*, described in detail in Section 1.1 below.

This application of the classical theory of changepoint detection to classification is novel, but the classification setting lends itself well to the methodology. Classification methods typically require training data, which we leverage to construct our detection procedure. While we focus on the binary classification setting, which is the simplest and most common, the same ideas extend to label-shift in multi-class classification.

---

\*clevans@andrew.cmu.edu

†mgsell@andrew.cmu.edu

## 1.1 Changepoints and label shift

Let  $\mathbb{P}_\infty$  and  $\mathbb{P}_0$  denote the pre- and post- change distributions of the data  $(X_i, Y_i)$ , and  $\nu \geq 0$  denote the **changepoint** in the sequence, such that

$$\begin{aligned} (X_1, Y_1), \dots, (X_\nu, Y_\nu) &\stackrel{iid}{\sim} \mathbb{P}_\infty \\ (X_{\nu+1}, Y_{\nu+1}), (X_{\nu+2}, Y_{\nu+2}), \dots &\stackrel{iid}{\sim} \mathbb{P}_0. \end{aligned} \tag{1}$$

We also assume a separate training data set  $(X'_1, Y'_1), \dots, (X'_{n_{train}}, Y'_{n_{train}}) \sim P_\infty$  is available. Throughout the paper we use the subscripts  $\infty$  and  $0$  for pre- and post-change quantities respectively, to be consistent with the sequential changepoint detection literature. The motivation is that  $\nu = \infty$  indicates the change never occurs, so data is from the pre-change distribution, while  $\nu = 0$  indicates the change occurs before we observe any data, so data is from the post-change distribution. With some abuse of notation, when context is clear we will let  $\mathbb{P}_\infty$  and  $\mathbb{P}_0$  denote general pre- and post-change distributions, so for example  $(X_i, Y_i) \sim \mathbb{P}_\infty$  and  $X_i \sim \mathbb{P}_\infty$  both indicate data drawn before a change occurs.

Arbitrary changes to high-dimensional classification data may be impossible to detect, so it is necessary to make additional assumptions on the nature of the change. We will focus on the **label shift** setting (Saerens et al., 2002; Storkey, 2009), which has received recent attention in the machine learning literature (Ackerman et al., 2020; Azizzadenesheli et al., 2019; Lipton et al., 2018; Rabanser et al., 2019). Label shift assumes that the marginal distribution of  $Y_i$  changes, but the conditional distribution of  $X_i|Y_i$  does not:

**Assumption 1.** *(Label shift) Let  $f_{\infty, X, Y}$ ,  $f_{\infty, Y}$ , and  $f_{\infty, X|Y=y}$  denote the densities/mass functions of  $(X_i, Y_i)$ ,  $Y_i$ , and  $X_i|Y_i = y$  respectively, under  $\mathbb{P}_\infty$ . Similarly define  $f_{0, X, Y}$ ,  $f_{0, Y}$ , and  $f_{0, X|Y=y}$ . The label shift assumption is that  $f_{0, X|Y=y} \equiv f_{\infty, X|Y=y}$  for all  $y$ , so*

$$f_{0, X, Y}(x, y) = f_{0, Y}(y) f_{0, X|Y=y}(x) = f_{0, Y}(y) f_{\infty, X|Y=y}(x) \quad \forall x, y. \tag{2}$$

The intuition for label shift is that the characteristics of an observation within each class do not change, but the distribution of classes change. Note that label shift is in contrast with *covariate shift*, another form of distributional change considered in the literature which assumes that  $f_{0, Y|X=x} \equiv f_{\infty, Y|X=x}$  for all  $x$  (Gretton et al., 2009; Shimodaira, 2000; Sugiyama et al., 2008).

## 1.2 Changepoints and classifier scores

After training the classifier  $\mathcal{A}$ , we sequentially observe new observations  $X_1, X_2, X_3, \dots$  with unknown labels, and make a prediction  $S_i := \mathcal{A}(X_i)$  for each new observation. Under the label shift assumption, the pre- and post-change marginal densities of  $X_i$  can be written as a mixture of the same components, but with different mixing parameters:

$$\begin{aligned} f_{\infty, X}(x) &= \pi_\infty f_{\infty, X|Y=1}(x) + (1 - \pi_\infty) f_{\infty, X|Y=0}(x) \\ f_{0, X}(x) &= \pi_0 f_{\infty, X|Y=1}(x) + (1 - \pi_0) f_{\infty, X|Y=0}(x), \end{aligned} \tag{3}$$

where  $\pi_\infty = P_\infty(Y_i = 1)$  and  $\pi_0 = P_0(Y_i = 1)$ . Label shift is therefore reflected directly in the marginal distribution of  $X_i$  in the observed sequence. Furthermore, as discussed in Section 1.4.1, optimal changepoint detection methods for the sequence  $X_1, X_2, X_3, \dots$  are functions of the likelihood ratio  $f_{0, X}(X_i)/f_{\infty, X}(X_i)$  if it is known. When the densities  $f_{\infty, X|Y=1}$  and  $f_{\infty, X|Y=0}$  are known, it is therefore straightforward to apply classic sequential changepoint results to the label shift setting.

However, the densities  $f_{\infty, X|Y}$  are usually unknown. With a small number of covariates, nonparametric density estimation procedures may be feasible, but classifiers often rely on a large number of features.

**Classifier scores as approximations of the optimal  $P(Y_i = 1|X_i)$ .** To reduce the dimensionality of the observed data, note that under the label shift assumption, we can rewrite the likelihood ratio as

$$\frac{f_{0,X}(X_i)}{f_{\infty,X}(X_i)} = \frac{\pi_0}{\pi_\infty} P_\infty(Y_i = 1|X_i) + \frac{1 - \pi_0}{1 - \pi_\infty} (1 - P_\infty(Y_i = 1|X_i)). \quad (4)$$

As a function of  $X_i$  and with  $\pi_0 \neq \pi_\infty$ , this likelihood ratio is linear in  $P(Y_i = 1|X_i)$ . If  $S_i$  is a good approximation to  $P_\infty(Y_i = 1|X_i)$ , then changepoint procedures that are a function of  $X_i$  through the likelihood ratio can be replaced by procedures that are a function of the classifier scores  $S_i$  directly. In fact, under the label shift assumption, if  $S_i = P(Y_i = 1|X_i)$ , it can be shown that (4) is exactly the likelihood ratio of the scores  $S_i$ . However, in practice  $S_i \neq P(Y_i = 1|X_i)$ , so rather than rely on this equality as the foundation for our procedure, we merely use this relationship as inspiration to reduce dimension by focusing on changepoints that are reflected in the distribution of classifier scores  $S_i$ . Section 1.3 develops this further.

**Classifier scores as maximizers of differences in distribution.** Beyond the argument above that relies on  $P_\infty(Y_i = 1|X_i) \approx S_i$ , there is another motivation for using classifier scores  $S_i$  as a dimension reduction for label shift detection. Consider any summary  $Z_i$  that is a function of  $X_i$ , the classifier score  $S_i$  being one such example. Because  $Z_i$  is a function only of  $X_i$ , the same label shift assumption holds directly for  $Z_i$ . That is, if  $f_\infty$ ,  $f_\infty^1$ , and  $f_\infty^0$  are the respective densities of  $Z_i$ ,  $Z_i|Y_i = 1$ , and  $Z_i|Y_i = 0$  under  $\mathbb{P}_\infty$ , and  $f_0$  is the density of  $Z_i$  under  $\mathbb{P}_0$ , then

$$\begin{aligned} f_\infty(z) &= \pi_\infty f_\infty^1(z) + (1 - \pi_\infty) f_\infty^0(z) \\ f_0(z) &= \pi_0 f_\infty^1(z) + (1 - \pi_0) f_\infty^0(z). \end{aligned} \quad (5)$$

Then applying Pinsker's inequality gives

$$KL(f_0, f_\infty) \geq 2(\pi_0 - \pi_\infty)^2 TV^2(f_\infty^1, f_\infty^0). \quad (6)$$

As we summarize in Section 1.4.1, the performance of sequential changepoint detection procedures often depends on the KL divergence between the pre- and post-change distributions (Lorden, 1971), with a greater KL divergence corresponding to improved detection ability. (6) shows that this divergence is guaranteed to be large when the total variation between the class-conditional densities  $f_\infty^1$  and  $f_\infty^0$  is large. Since classification scores are essentially constructed to maximize the difference between these two distributions, using  $Z_i = S_i$  should naturally lead to good changepoint detection performance. In Section 3, we show in simulations how improving classifier performance also improves the performance of changepoint detection procedures that use classifier scores.

We close this section with a simple illustration of label shift and its consequences for the distribution of classifier scores.

**Example:** Figure 1 shows a simple example of label shift, with data generated as

$$\begin{aligned} Y &\sim \text{Bernoulli}(\pi_\infty) \text{ (pre-change)} & Y &\sim \text{Bernoulli}(\pi_0) \text{ (post-change)} \\ X|Y=0 &\sim N(\boldsymbol{\mu}_0, \boldsymbol{\Sigma}) & X|Y=1 &\sim N(\boldsymbol{\mu}_1, \boldsymbol{\Sigma}) \\ X|Y=1 &\sim N(\boldsymbol{\mu}_1, \boldsymbol{\Sigma}). \end{aligned} \quad (7)$$

For simplicity, this example uses the scores from Linear Discriminant Analysis (LDA), which have closed form:

$$S_i = \frac{\widehat{\pi}_\infty \text{MVN}(X_i; \widehat{\boldsymbol{\mu}}_1, \widehat{\boldsymbol{\Sigma}})}{\widehat{\pi}_\infty \text{MVN}(X_i; \widehat{\boldsymbol{\mu}}_1, \widehat{\boldsymbol{\Sigma}}) + (1 - \widehat{\pi}_\infty) \text{MVN}(X_i; \widehat{\boldsymbol{\mu}}_0, \widehat{\boldsymbol{\Sigma}})}, \quad (8)$$

where  $\text{MVN}(\cdot; \boldsymbol{\mu}, \boldsymbol{\Sigma})$  denotes the multivariate normal density with mean  $\boldsymbol{\mu}$  and covariance matrix  $\boldsymbol{\Sigma}$ .

The density of LDA scores for each class is

$$f_\infty^i(s) = \left( \frac{1}{s - s^2} \right) \phi \left( \frac{\log \left( \frac{s(1 - \widehat{\pi}_\infty)}{(1 - s)\widehat{\pi}_\infty} \right) + \frac{1}{2} \left( \widehat{\boldsymbol{\mu}}_1^T \widehat{\boldsymbol{\Sigma}}^{-1} \widehat{\boldsymbol{\mu}}_1 - \widehat{\boldsymbol{\mu}}_0^T \widehat{\boldsymbol{\Sigma}}^{-1} \widehat{\boldsymbol{\mu}}_0 \right) - \boldsymbol{\mu}_i^T \widehat{\boldsymbol{\Sigma}}^{-1} (\widehat{\boldsymbol{\mu}}_1 - \widehat{\boldsymbol{\mu}}_0)}{\sqrt{(\widehat{\boldsymbol{\mu}}_1 - \widehat{\boldsymbol{\mu}}_0)^T \widehat{\boldsymbol{\Sigma}}^{-1} \boldsymbol{\Sigma} \widehat{\boldsymbol{\Sigma}}^{-1} (\widehat{\boldsymbol{\mu}}_1 - \widehat{\boldsymbol{\mu}}_0)}} \right), \quad (9)$$

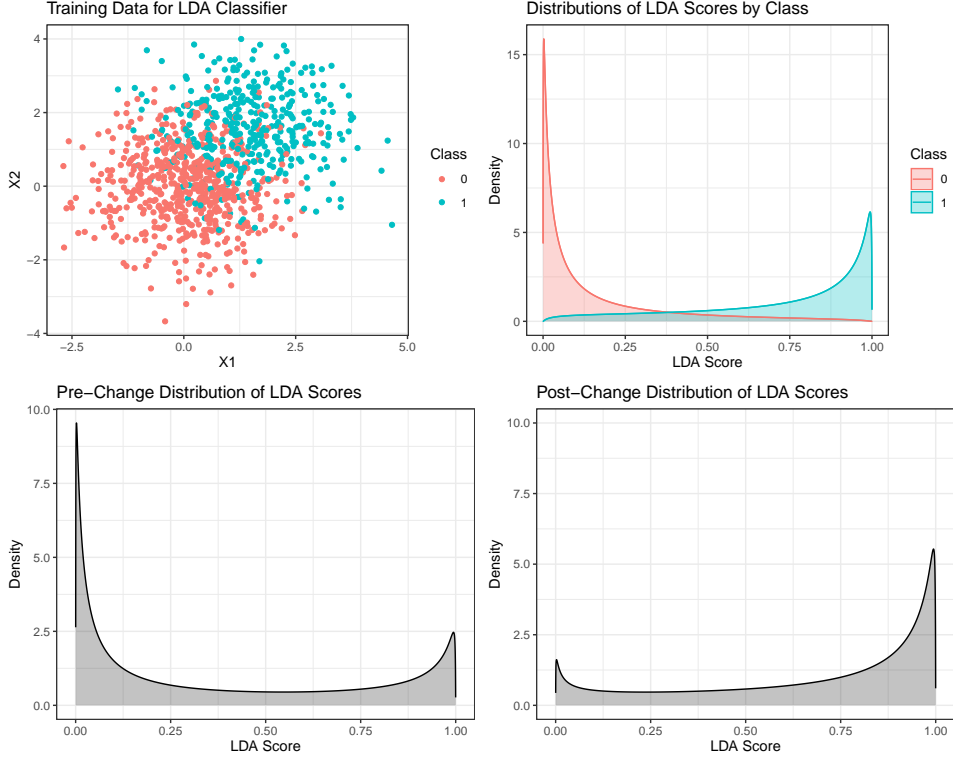


**Figure 1:** Example of label shift. Top left: Raw classification data come from a mixture of bivariate Gaussians (7), with  $\mu_0 = \mathbf{0}$ ,  $\mu_1 = [1.5, 1.5]^T$ , and  $\Sigma = \mathbf{I}$ . Top right: An LDA classifier is trained, with LDA scores given by (8). The distribution of LDA scores is shown, where the exact expression for each density is given by (9). Bottom left: The pre-change distribution of LDA scores, when  $\pi_\infty = 0.4$ . Bottom right: The post-change distribution of LDA scores, when  $\pi_0 = 0.9$ . For illustrative purposes, the change from  $\pi_\infty$  to  $\pi_0$  shown in this figure is more extreme than what we consider in simulations.

where  $i = 0, 1$  and  $\phi$  is the standard normal density.

If each part of (5) were known, existing optimal changepoint detection procedures (e.g., (Page, 1954)) could be applied. Similarly, if  $\pi_0$  and/or  $\pi_\infty$  were unknown, but the conditional densities  $f_\infty^1$  and  $f_\infty^0$  were known, we could apply changepoint detection procedures that allow for unknown parameters (e.g., (Lai, 1998; Mei, 2006; Unnikrishnan et al., 2011)). As motivation, we briefly discuss those cases in Section 2. However, in the typical case where the conditional densities are unknown, a nonparametric detection method is required.

### 1.3 Nonparametric changepoint procedures under label shift

In the case where the conditional densities of 5 are unknown, a nonparametric approach is needed. The focus of this manuscript will be on the development and study of simple nonparametric procedures that replace the conditional densities in (5) with density estimates based on the training data.

Estimates of the conditional densities  $f_\infty^1$  and  $f_\infty^0$  depend on the labeled classifier scores  $\mathbf{S}^* = (S_1^*, Y_1^*), \dots, (S_{n_{est}}^*, Y_{n_{est}}^*) = (\mathcal{A}(X_1^*), Y_1^*), \dots, (\mathcal{A}(X_{n_{est}}^*), Y_{n_{est}}^*)$  from a pre-change sample of size  $n_{est}$ , which we will use in estimating the pre- and post-change score distributions. For theoretical simplicity, we consider this *estimation sample* to be an independent sample from the *training sample* used to estimate  $\mathcal{A}(\cdot)$  above. In practice, a variety of sample-splitting or cross-validation procedures could be considered to produce these two data sets from a single pre-detection data set.

Since our methods depend on the random estimation sample  $\mathbf{S}^*$  through the estimated densities  $\hat{f}_\infty^1$  and  $\hat{f}_\infty^0$ , the operating characteristics of our proposed procedures are random. When  $\|\hat{f}_\infty^1 - f_\infty^1\|_\infty$  and  $\|\hat{f}_\infty^0 - f_\infty^0\|_\infty$  are both close to 0, we can expect the performance of our nonparametric procedures to be close to the performance of the detection procedure that uses the true  $f_\infty^1$  and  $f_\infty^0$ . Throughout this manuscript we will refer to the procedure using  $f_\infty^1$  and  $f_\infty^0$  as the *optimal* detection procedure, in the sense that it is optimal for detecting changes to the classifier scores  $S_i$ . However, it is important to remember that this “optimal” procedure depends on the performance of the classifier  $\mathcal{A}(\cdot)$ , as we remarked in Section 1.2, and so may not be optimal for detecting a change to the distribution of  $X_i$  if a poor classifier is used.

We will show that the operating characteristics of these procedures are consistent for the operating characteristics of the optimal procedure based on the true conditional densities  $f_\infty^1$  and  $f_\infty^0$ . We consider three different scenarios for the pre- and post-change parameters  $\pi_\infty$  and  $\pi_0$ : when  $\pi_\infty$  and  $\pi_0$  are both known or can be consistently estimated outside of the changepoint procedure; when  $\pi_\infty$  can be estimated but  $\pi_0$  is unknown; and when  $\pi_\infty$  and  $\pi_0$  both cannot be estimated.

The remainder of this manuscript focuses on further developing and supporting the nonparametric procedures based on density estimation. Section 1.4 describes additional background and related literature. Section 2 presents the procedures in detail and the theoretical results that support them. In Section 3, we present a detailed simulation study to evaluate the performance of our approach in practice and in the context of the existing literature.

## 1.4 Background and related literature

The methods developed in this paper are inspired by ideas from three different areas. Parametric changepoint detection provides optimal detection procedures, under strong assumptions about the pre- and post-change distributions. Nonparametric changepoint detection aims to weaken these assumptions, but the cost is often the optimality of the procedure. Previous literature on label shift provides methods for batch detection, but there has been less work on sequential detection. Our work aims to develop a nonparametric procedure that approaches the performance of parametric methods, for detecting label shift in sequential data.

### 1.4.1 Parametric Changepoint Detection

Classical sequential changepoint detection procedures, such as CUSUM (Moustakides, 1986; Page, 1954) and the Shiryaev-Roberts procedure and its modifications (Roberts, 1966; Shiryaev, 2007; Tartakovsky et al., 2012a) assume that the pre- and post-change distributions are known. These procedures rely on the observed likelihood ratios  $f_{0,X}(X_i)/f_{\infty,X}(X_i)$  to define a stopping time  $T$  for the sequence  $\{X_i\}$ . The performance of  $T$  when a change occurs at time  $\nu$  is measured by the detection delay, with popular choices being Lorden’s (Lorden, 1971) and Pollak’s (Pollak, 1985):

$$\text{Lorden's detection delay for stopping time } T: \sup_{0 \leq \nu < \infty} \text{ess sup } \mathbb{E}_\nu[(T - \nu)^+ | X_1, \dots, X_\nu], \quad (10)$$

$$\text{Pollak's detection delay for stopping time } T: \sup_{0 \leq \nu < \infty} \mathbb{E}_\nu[T - \nu | T \geq \nu]. \quad (11)$$

The aim in designing  $T$  is to minimize detection delay while maintaining control on the rate of false alarms, captured by requiring the average run length to false alarm  $\mathbb{E}_\infty(T) \geq \gamma$  for a choice of  $\gamma > 0$ . While Lorden’s and Pollak’s detection delays appear difficult to calculate, the supremum occurs at  $\nu = 0$  for CUSUM-based procedures that are initialized at 1. That is,  $\mathbb{E}_0(T)$  is equivalent to both Lorden and Pollak’s criteria for CUSUM (Tartakovsky et al., 2014). For Shiryaev-Roberts initialized at 0,  $\mathbb{E}_0(T)$  is equivalent to Pollak’s criterion (Tartakovsky et al., 2014).

Moustakides (1986) showed that CUSUM is exactly optimal for Lorden’s criterion, while Tartakovsky et al. (2012a) showed that a modification of the Shiryaev-Roberts procedure is third-order asymptotically optimal

for Pollak's criterion. In either case, when  $E_\infty(T) \approx \gamma$ , then the detection delay behaves asymptotically like

$$\frac{\log \gamma}{KL(f_0, f_\infty)} \tag{12}$$

as  $\gamma \rightarrow \infty$ , where  $KL(f_0, f_\infty)$  is the KL divergence.

Under the strong assumption that the changepoint  $\nu$  is the only unknown, optimality or asymptotic optimality can be achieved, but in practice such assumptions are often unreasonable. For our purposes, while we may have previous observations from the pre-change distributions, we are unlikely to have post-change data before the change occurs.

To address this issue, there has been much work on relaxing the strict assumptions of a fully specified post-change distribution. A common assumption is that the post-change distribution is known up to some parameter, with a specified parameter space. One can then either maximize (the generalized likelihood ratio (GLR) approach; see, e.g., Siegmund and Venkatraman (1995)) or mix (see, e.g., Lai (1998)) over the unknown post-change parameter. For cases when both the pre- and post-change distributions are unknown but can be parameterized (they need not belong to the same family), Mei (2006) proposes a procedure that maximizes over the pre-change parameter and mixes over the post-change parameter. Alternatively, when the pre-change and/or post-change parameter are unknown, one can attempt to find a *least favorable pair* for the distributions (Unnikrishnan et al., 2011), which gives a worst-case detection delay for a specified average run length to false alarm (ARL)  $E_\infty(T)$ .

In the label shift setting we consider in this paper, the conditional densities  $f_\infty^1$  and  $f_\infty^0$  are unknown, but can be estimated from a pre-change estimation sample  $\mathbf{S}^*$ . This allows us to define nonparametric versions of detection procedures like CUSUM (Page, 1954), Lai's mixture procedure (Lai, 1998), and Unnikrishnan *et al.*'s least favorable pair (Unnikrishnan et al., 2011). Our nonparametric procedures have operating characteristics which are consistent for those of the original versions, but do not require us to know  $f_\infty^1$  and  $f_\infty^0$  exactly.

#### 1.4.2 Nonparametric Changepoint Detection

Other authors have proposed a variety of nonparametric detection procedures. One group of methods replaces the likelihood ratio  $f_{0,X}(X_i)/f_{\infty,X}(X_i)$  with a rank-based likelihood ratio or score function  $g(X_i)$ , then proceeds as usual with a procedure like CUSUM or Shiryaev-Roberts. The function  $g(\cdot)$  is designed to detect specific types of expected changes, such as the mean or variance (Brodsky and Darkhovsky, 1993, 2000; Tartakovsky et al., 2012b, 2006a,b), or a change to a stochastically larger/smaller distribution (Bell et al., 1994; Gordon and Pollak, 1994, 1995; McDonald, 1990). Another tactic is to replace the likelihood ratio  $f_{0,X}(X_i)/f_{\infty,X}(X_i)$  with an estimate. For example, Baron (2000) estimates the post-change distribution online with a histogram density estimator. Other authors consider estimating the likelihood ratio directly, and using the estimated ratio to approximate the KL divergence or PE divergence (Kawahara and Sugiyama, 2009; Liu et al., 2013). When the approximate divergence gets large (suggesting a change has occurred), the procedure raises an alarm. Rather than substitute the likelihood ratio, other work has adapted nonparametric tests for differences in distribution. For example, Madrid Padilla et al. (2019) adapt a Kolmogorov-Smirnov test to the sequential setting and use the test for anomaly detection. Repeated retrospective tests such as *t*-tests (Hawkins et al., 2003) and Cramer-von-Mises tests (Ross and Adams, 2012) have also been used for sequential detection. For high dimensional data, Chen (2019) and Chu and Chen (2018) apply a nonparametric test based on nearest-neighbors graphs. An advantage of this method is that multivariate data can be handled, assuming we can define an appropriate distance between observations for use in nearest-neighbor graphs, and the null distribution should be the same regardless of the data-generating process.

As in Baron (2000), Kawahara and Sugiyama (2009), and Liu et al. (2013), in this paper we focus on estimating the likelihood ratio. However, previous research has considered the general changepoint setting

rather than the specific label shift case. By using the label shift assumption, we can estimate the likelihood ratio through estimates of  $\hat{f}_\infty^1$  and  $\hat{f}_\infty^0$ . As we discuss in Section 2.1, using the form of the likelihood ratio under label shift (5) provides useful properties to the estimated likelihood ratio function, which allows us to derive theoretical guarantees on our methods' performance. We show through simulations (Section 3 and Appendix A.6) that our methods outperform those which estimate the likelihood ratio without the label-shift assumption.

### 1.4.3 Label Shift Detection and Adaptation

Methods for adapting classifiers to label shift have been proposed by several authors, in the non-sequential setting where the classifier is to be applied to a new test dataset. For example, Saerens et al. (2002) propose using the EM algorithm to iteratively adjust probabilities to maximize the likelihood of the test data, while Storkey (2009) suggests specifying a prior distribution on the marginal distribution of  $Y_i$  and updating the prior using the observed covariates of the test data. Confusion matrices are used by Lipton et al. (2018) to estimate importance weights  $P_0(Y_i = 1)/P_\infty(Y_i = 1)$ , which can then be used to correct predictions. Azizzadenesheli et al. (2019) note that this method works well for large samples, but the weight estimation is hard to use and control with smaller sample sizes. Instead, Azizzadenesheli et al. (2019) propose weight estimation with regularization to avoid these issues.

For detecting label shift, non-sequential two-sample tests between training and test data have been proposed. A likelihood ratio test, based on the likelihood maximized by EM, is proposed by Saerens et al. (2002). In Lipton et al. (2018), the authors note that label shift implies a change in the distribution of classifier predictions, so a two-sample test comparing the training and test predictions is suitable for detecting a change. This is expanded by Rabanser et al. (2019), who consider possibilities for dimension-reduction to apply two-sample tests to high-dimensional data. One possibility is the label shift test proposed by Lipton et al. (2018), which works reasonably well even when the label-shift assumption is not met. For sequential detection of label shift, Ackerman et al. (2020) implement the nonparametric detection procedure in Ross and Adams (2012) based on repeated Cramer–von-Mises tests for a change in distribution, using the `cpm` package (Ross, 2015) in R.

Like Ackerman et al. (2020), we consider the problem of detecting label shift in a sequential setting, rather than a batch setting. However, in contrast to Ackerman et al. (2020), we aim to use the label-shift assumption directly in our detection procedures by estimating  $f_\infty^1$  and  $f_\infty^0$ . By estimating the likelihood ratio and using the label-shift assumption, our proposed approach outperforms the nonparametric method in Ackerman et al. (2020) (see Appendix A.6).

## 2 Label shift detection with density estimation

As shown in (5), the label-shift assumption allows a general change in the score distributions to be reduced to a change in the mixing parameter of the two conditional score densities  $f_\infty^1$  and  $f_\infty^0$ . If the conditional score densities  $f_\infty^1$  and  $f_\infty^0$  were known, a variety of classical detection procedures could be used, depending on assumptions on  $\pi_\infty$  and  $\pi_0$ . In practice, the assumption that  $f_\infty^1$  and  $f_\infty^0$  are known is likely unreasonable, so we generalize those procedures by substituting density estimates. In this section we discuss resulting detection procedures under each scenario for  $\pi_\infty$  and  $\pi_0$ .

Section 2.1, addresses the case where  $\pi_0$  is known. Estimates  $\hat{\pi}_\infty$ ,  $\hat{f}_\infty^1$ , and  $\hat{f}_\infty^0$  from an estimation sample  $\mathbf{S}^*$  can be substituted to produce an approximate CUSUM detection procedure which is asymptotically optimal as  $n_{est} \rightarrow \infty$ . Section 2.2 follows Lai (1998) to handle unknown  $\pi_0$  by mixing over possible values of  $\pi_0$ . By substituting  $\hat{\pi}_\infty$ ,  $\hat{f}_\infty^1$ , and  $\hat{f}_\infty^0$ , we produce a procedure with operating characteristics consistent for those of Lai's mixture rule as  $n_{est} \rightarrow \infty$ . Finally, Section 2.3 addresses both unknown  $\pi_\infty$  and  $\pi_0$  using the least favorable distribution approach from Unnikrishnan et al. (2011). As in Section 2.2, our estimated procedure

achieves operating rules consistent for Unnikrishnan *et al.*'s least favorable operating characteristics.

## 2.1 Density estimation with known $\pi_0$

Let  $\lambda(s) = \frac{f_0(s)}{f_\infty(s)}$  be the likelihood ratio function for a change in the distribution of the classifier scores  $S_i$ . The optimal CUSUM changepoint detection procedure (Moustakides, 1986; Page, 1954) is defined by a detection statistic  $R_t$  and a stopping time  $T_{CS}(A)$  with threshold  $A$ :

$$R_t = \max_{1 \leq k \leq t} \prod_{i=k}^t \lambda(S_i) \quad T_{CS}(A) = \inf\{t \geq 1 : R_t \geq A\}. \quad (13)$$

The detection statistic  $R_t$  accumulates evidence for a change until it crosses the cutoff  $A$ , at which point a change in distribution is declared.

Let  $\mathbf{S} = S_1, S_2, \dots$ . Throughout this section, we will denote expectation with respect to  $\mathbf{S}$  as  $\mathbb{E}_{\mathbf{S}}$ , which may be under either  $\mathbb{P}_\infty$  or  $\mathbb{P}_0$ . The operating characteristics of the CUSUM procedure are defined by  $\mathbb{E}_{\mathbf{S}}(T_{CS}(A))$ , where  $\mathbf{S} \sim \mathbb{P}_\infty$  for the Average Run Length and  $\mathbf{S} \sim \mathbb{P}_0$  for the detection delay. Our results hold under both distributions, so we will leave it unspecified throughout Section 2 unless necessary.

Consider an estimate  $\hat{\lambda}$  of the likelihood ratio function, based on our estimation sample  $\mathbf{S}^* = (S_1^*, Y_1^*), \dots, (S_{n_{est}}^*, Y_{n_{est}}^*)$ . A natural nonparametric CUSUM procedure simply replaces  $\lambda$  in the optimal procedure with  $\hat{\lambda}$ , to define a detection statistic  $\tilde{R}_t$  and a stopping time  $\tilde{T}_{CS}(A)$ :

$$\tilde{R}_t = \max_{1 \leq k \leq t} \prod_{i=k}^t \hat{\lambda}(S_i) \quad \tilde{T}_{CS}(A) = \inf\{t \geq 1 : \tilde{R}_t \geq A\}. \quad (14)$$

The operating characteristics of the CUSUM procedure in (14) depend on the estimation sample  $\mathbf{S}^*$ , which we make explicit with the notation  $\mathbb{E}_{\mathbf{S}|\mathbf{S}^*}(\tilde{T}_{CS}(A))$ . Our goal is to show that

$$\mathbb{E}_{\mathbf{S}|\mathbf{S}^*}(\tilde{T}_{CS}(A)) \xrightarrow{P} \mathbb{E}_{\mathbf{S}}(T_{CS}(A)) \quad (15)$$

under both  $\mathbb{P}_\infty$  and  $\mathbb{P}_0$  as  $n_{est} \rightarrow \infty$ . Our main result is Theorem 1, which provides sufficient conditions for the convergence in (15). In the remainder of this section, we construct a specific estimate of  $\lambda$ , using the label-shift assumption, which satisfies the requirements in Theorem 1.

**Theorem 1.** *Let  $\hat{\lambda}$  be an estimate of the likelihood ratio function  $\lambda$ , depending on an estimation sample  $\mathbf{S}^*$  of size  $n_{est}$ . Suppose that there exist bounds  $l_\lambda, u_\lambda \in (0, \infty)$  such that  $l_\lambda \leq \lambda(s) \leq u_\lambda$  for all  $s \in \text{supp}(S_i)$ , and  $P_{\mathbf{S}^*}(l_\lambda \leq \hat{\lambda}(s) \leq u_\lambda \quad \forall s \in \text{supp}(S_i)) \rightarrow 1$  as  $n_{est} \rightarrow \infty$ . Further, let  $\{\mathcal{S}_c\}_{c \in (0, \infty)}$  be a collection of sets such that for all  $c > 0$ ,*

$$\sup_{s \in \mathcal{S}_c} |\hat{\lambda}(s) - \lambda(s)| \xrightarrow{P} 0 \quad (16)$$

*as  $n_{est} \rightarrow \infty$ , and  $\lim_{c \rightarrow 0} P_{\mathbf{S}^*}(S_i \in \mathcal{S}_c) = 1$ . Finally, suppose that  $\mathbb{E}_{\mathbf{S}}(T_{CS}(A))$  is a continuous function of  $A$ . Then for given  $A$ , for all  $\eta > 0$  we have*

$$P_{\mathbf{S}^*} \left( |\mathbb{E}_{\mathbf{S}|\mathbf{S}^*}(\tilde{T}_{CS}(A)) - \mathbb{E}_{\mathbf{S}}(T_{CS}(A))| < \eta \right) \rightarrow 1 \quad (17)$$

*as  $n_{est} \rightarrow \infty$ .*

*Proof.* See Appendix A.2. □

Theorem 1 gives conditions under which the operating characteristics of the nonparametric procedure with stopping time  $\tilde{T}_{CS}(A)$  are consistent, as  $n_{est} \rightarrow \infty$ . Here  $\hat{\lambda}$  represents a generic estimate of the likelihood function  $\lambda$ . In principle, any method for estimating the likelihood ratio could be used, such as those discussed in Kawahara and Sugiyama (2009) and Liu et al. (2013), so long as the necessary data is available and the requirements of Theorem 1 can be shown. However, the label-shift assumption lends itself to a natural estimate  $\hat{\lambda}_L$  that satisfies Theorem 1.

Using the estimation sample  $\mathbf{S}^*$ , suppose that we obtain some estimates  $\hat{\pi}_\infty$ ,  $\hat{f}_\infty^0$ , and  $\hat{f}_\infty^1$ . Under the label-shift assumption, these can be combined to form a plug-in likelihood ratio estimate,

$$\hat{\lambda}_L(s) = \frac{\hat{f}_0(s)}{\hat{f}_\infty(s)} = \frac{\pi_0 \hat{f}_\infty^1(s) + (1 - \pi_0) \hat{f}_\infty^0(s)}{\hat{\pi}_\infty \hat{f}_\infty^1(s) + (1 - \hat{\pi}_\infty) \hat{f}_\infty^0(s)}, \quad (18)$$

where we use the subscript  $L$  (for ‘‘label shift’’, to emphasize that we leverage the label-shift assumption) to distinguish the estimator in (18) from the generic  $\hat{\lambda}$  in Theorem 1. In this section, we will assume  $\pi_0$  is known or can be consistently estimated; in Section 2.2 and 2.3 we will address the case where  $\pi_0$  is unknown and cannot be estimated.

To show that  $\hat{\lambda}_L$  satisfies the conditions of Theorem 1, we require the following:

1. Uniform convergence of  $\hat{\lambda}_L$  to  $\lambda$  on each  $\mathcal{S}_c$ ,
2. A bounded likelihood ratio function  $\lambda$ ,
3. That  $\hat{\lambda}_L$  is also bounded.

These conditions allow us to control  $\sup_{t \leq t_0} |\tilde{R}_t - R_t|$  for large  $t_0$ : upper and lower bounds on  $\lambda$  and  $\hat{\lambda}$  lead to bounds on  $\tilde{R}_t$  and  $R_t$ , while uniform convergence of  $\hat{\lambda}$  to  $\lambda$  controls  $|\tilde{R}_t - R_t|$ .

In the following lemma, we show that the estimate  $\hat{\lambda}_L$  from (18) converges uniformly to  $\lambda$ , provided the density estimates  $\hat{f}_\infty^1$  and  $\hat{f}_\infty^0$  converge in  $L_\infty$  to  $f_\infty^1$  and  $f_\infty^0$ . When  $f_\infty(s)$  is close to 0, it can be hard to ensure  $\hat{\lambda}_L(s)$  is close to  $\lambda(s)$ , so we focus only on  $s$  for which  $f_\infty(s) > c > 0$ . For  $\hat{\lambda}_L$ , the sets  $\mathcal{S}_c$  from Theorem 1 are then  $\mathcal{S}_c = \{s : f_\infty(s) > c\}$ . It is clear that  $\lim_{c \rightarrow 0} P_{\mathbf{S}}(S_i \in \mathcal{S}_c) = 1$ , so it remains to demonstrate uniform convergence in probability on each  $\mathcal{S}_c$ .

**Lemma 1.** *Suppose that  $\hat{\pi}_\infty \xrightarrow{P} \pi_\infty \in (0, 1)$ , and  $\pi_0 \in (0, 1)$ . Let  $c > 0$  and  $\mathcal{S}_c = \{s : f_\infty(s) > c\}$ , and suppose that  $\hat{f}_\infty^1$  and  $\hat{f}_\infty^0$  are estimates such that*

$$\sup_{s \in \mathcal{S}_c} |\hat{f}_\infty^0(s) - f_\infty^0(s)| \xrightarrow{P} 0 \quad \text{and} \quad \sup_{s \in \mathcal{S}_c} |\hat{f}_\infty^1(s) - f_\infty^1(s)| \xrightarrow{P} 0 \quad (19)$$

as  $n_{est} \rightarrow \infty$ , and  $f_\infty, f_0$  are bounded above. Then

$$\sup_{s \in \mathcal{S}_c} |\hat{\lambda}_L(s) - \lambda(s)| \xrightarrow{P} 0. \quad (20)$$

*Proof.* See Appendix A.1. □

**Remark:** The estimates  $\hat{f}_\infty^1$  and  $\hat{f}_\infty^0$  in (18) can be any density estimates that satisfy Lemma 1. A natural choice is to use kernel density estimation;  $L_\infty$ -convergence of kernel density estimates can be achieved under certain assumptions on the density and the bandwidth (see, for example, Giné and Guillou (2002)). For bounded densities (e.g., score distributions bounded to  $[0, 1]$ ), the Beta kernel density estimate (Chen, 1999) also converges in  $L_\infty$  (Bouezmarni and Rolin, 2003).

In addition to convergence of  $\hat{\lambda}_L$  to  $\lambda$ , we require bounds on  $\lambda$  and  $\hat{\lambda}_L$  for Theorem 1. Under the label-shift assumption,

$$\begin{aligned} \min \left\{ \frac{\pi_0}{\pi_\infty}, \frac{1-\pi_0}{1-\pi_\infty} \right\} &\leq \lambda(s) \leq \max \left\{ \frac{\pi_0}{\pi_\infty}, \frac{1-\pi_0}{1-\pi_\infty} \right\}, & \forall s \in \text{supp}(S_i) \\ \min \left\{ \frac{\pi_0}{\hat{\pi}_\infty}, \frac{1-\pi_0}{1-\hat{\pi}_\infty} \right\} &\leq \hat{\lambda}_L(s) \leq \max \left\{ \frac{\pi_0}{\hat{\pi}_\infty}, \frac{1-\pi_0}{1-\hat{\pi}_\infty} \right\}, & \forall s \in \text{supp}(S_i). \end{aligned} \quad (21)$$

Provided  $\hat{\pi}_\infty$  converges, we can replace the bounds on  $\hat{\lambda}_L$  with bounds that do not depend on the specific value of  $\hat{\pi}_\infty$ . Let  $0 < \xi < \min\{\pi_\infty, 1 - \pi_\infty\}$ . If  $|\hat{\pi}_\infty - \pi_\infty| < \xi$ , then

$$\min \left\{ \frac{\pi_0}{\pi_\infty + \xi}, \frac{1-\pi_0}{1-\pi_\infty + \xi} \right\} \leq \hat{\lambda}_L(s) \leq \max \left\{ \frac{\pi_0}{\pi_\infty - \xi}, \frac{1-\pi_0}{1-\pi_\infty - \xi} \right\}, \quad \forall s \in \text{supp}(S_i). \quad (22)$$

When  $\hat{\pi}_\infty$  is consistent, then

$$P_{\mathbf{S}^*} \left( \min \left\{ \frac{\pi_0}{\pi_\infty + \xi}, \frac{1-\pi_0}{1-\pi_\infty + \xi} \right\} \leq \hat{\lambda}_L(s) \leq \max \left\{ \frac{\pi_0}{\pi_\infty - \xi}, \frac{1-\pi_0}{1-\pi_\infty - \xi} \right\}, \quad \forall s \in \text{supp}(S_i) \right) \rightarrow 1 \quad (23)$$

as  $n_{est} \rightarrow \infty$ .

Therefore,  $\hat{\lambda}_L$  as defined in (18) satisfies the requirements for Theorem 1 under some mild assumptions on  $f_\infty^1$ ,  $f_\infty^0$ ,  $\pi_\infty$ , and  $\pi_0$ . In particular, kernel density estimation for  $f_\infty^1, f_\infty^0$  tends to satisfy these. The two key properties we require for Theorem 1 are the boundedness of  $\hat{\lambda}_L$ , and its uniform convergence to  $\lambda$  on each set  $\mathcal{S}_c$ . Other estimates of  $\lambda$  might not satisfy these requirements, and we show in simulations in Section 3 that estimates of  $\lambda$  which do not leverage the label-shift assumption perform worse than our  $\hat{\lambda}_L$ .

## 2.2 Density estimation and mixtures over unknown $\pi_0$

Since a pre-change data set is already required for classifier training, it is reasonable to assume that we have data to estimate  $\pi_\infty$ ,  $f_\infty^0$ , and  $f_\infty^1$ . However, estimating the post-change mixing parameter  $\pi_0$  is often more difficult, as we are less likely to have post-change data or prior knowledge of the post-change parameter.

One approach to overcome an unknown  $\pi_0$  is to mix over a set  $\Pi_0$  of potential values for the post-change parameter, with a weight distribution  $w$ . Here we are inspired by the work of Lai (1998), who proves fairly general results. To deal with the computational complexity involved in the integration, Lai considers a window-limited approach that uses only a fixed number of the most recent observations. Let  $\Pi_0$  be the set of possible values for  $\pi_0$ , and let  $w(\pi_0)$  be a density on  $\Pi_0$ . Each potential  $\pi_0$  results in a different likelihood ratio function  $\lambda_{\pi_0}$ . Lai defines a CUSUM-type mixture stopping rule with detection statistic  $R_{t,w}$  and stopping time  $T_w(A)$  (Lai, 1998):

$$R_{t,w} = \max_{t-m_\alpha \leq k \leq t} \int_{\Pi_0} \prod_{i=k}^t \lambda_{\pi_0}(S_i) w(\pi_0) d\pi_0 \quad T_w(A) = \inf\{t \geq 1 : R_t \geq A\}, \quad (24)$$

where  $m_\alpha$  is the window size. Lai shows that  $T_w(A)$  is asymptotically optimal in  $\gamma$ . That is, for  $\pi_0 \in \Pi_0$ ,  $\pi_0 \neq \pi_\infty$ ,

$$\sup_{0 \leq \nu < \infty} \text{ess sup} \mathbb{E}_\nu[(T_w(A) - \nu)^+] | S_1, \dots, S_\nu] = \frac{\log A}{KL(f_0, f_\infty)} (1 + o(1)) \sim \frac{\log \gamma}{KL(f_0, f_\infty)} \quad (25)$$

as  $\gamma \rightarrow \infty$ . The asymptotic behavior of the detection delay in (25) is the same as the asymptotic behavior of the optimal CUSUM detection delay (12), so for large  $\gamma$  we would expect similar performance for Lai's mixture rule and the optimal CUSUM procedure.

In our label shift setting, we have

$$\lambda_{\pi_0}(s) = \frac{\pi_0 f_\infty^1(s) + (1 - \pi_0) f_\infty^0(s)}{\pi_\infty f_\infty^1(s) + (1 - \pi_\infty) f_\infty^0(s)}. \quad (26)$$

For each  $\pi_0$ , we can replace  $\lambda_{\pi_0}$  with its estimate:

$$\widehat{\lambda}_{\pi_0} = \frac{\widehat{f}_{\pi_0}}{\widehat{f}_\infty} = \frac{\pi_0 \widehat{f}_\infty^1(s) + (1 - \pi_0) \widehat{f}_\infty^0(s)}{\widehat{\pi}_\infty \widehat{f}_\infty^1(s) + (1 - \widehat{\pi}_\infty) \widehat{f}_\infty^0(s)}, \quad (27)$$

yielding the detection statistic  $\widetilde{R}_{t,w}$  and stopping time  $\widetilde{T}_w(A)$ :

$$\widetilde{R}_{t,w} = \max_{t-m_\alpha \leq k \leq t} \int_{\Pi_0} \prod_{i=k}^t \widehat{\lambda}_{\pi_0}(S_i) w(\pi_0) d\pi_0 \quad \widetilde{T}_w(A) = \inf\{t \geq 1 : \widetilde{R}_t \geq A\}. \quad (28)$$

Using the same arguments as in Lemma 1, we can show that if  $\widehat{\pi}_\infty \xrightarrow{p} \pi_\infty$ , and for all  $c > 0$

$$\sup_{s \in \mathcal{S}_c} |\widehat{f}_\infty^0(s) - f_\infty^0(s)| \xrightarrow{p} 0 \quad \sup_{s \in \mathcal{S}_c} |\widehat{f}_\infty^1(s) - f_\infty^1(s)| \xrightarrow{p} 0 \quad (29)$$

as  $n_{est} \rightarrow \infty$ , and  $f_\infty^1, f_\infty^0$  are bounded above, then

$$\sup_{\substack{s \in \mathcal{S}_c \\ \pi_0 \in \Pi_0}} |\widehat{\lambda}_{\pi_0}(s) - \lambda_{\pi_0}(s)| \xrightarrow{p} 0. \quad (30)$$

Furthermore, under the label-shift assumption the likelihood ratio is also bounded above, with an upper bound that does not depend on  $\pi_0$ :

$$\lambda_{\pi_0}(s) < \max \left\{ \frac{1}{\pi_\infty}, \frac{1}{1 - \pi_\infty} \right\} \quad \widehat{\lambda}_{\pi_0}(s) < \max \left\{ \frac{1}{\widehat{\pi}_\infty}, \frac{1}{1 - \widehat{\pi}_\infty} \right\} \quad \forall s \in \text{supp}(S_i). \quad (31)$$

This all suggests that operating characteristics for the nonparametric mixture procedure should also converge, and the proof looks very much like the proof of Theorem 1. However, the lower bound on  $\lambda_{\pi_0}$  does depend on  $\pi_0$ , so we will need to bound  $\pi_0$  away from 0 and 1 in the proof.

**Theorem 2.** *Let  $\Pi_0 = (a, b)$  where  $0 < a < b < 1$ . Suppose that  $\widehat{\pi}_\infty \xrightarrow{p} \pi_\infty \in (0, 1)$  as  $n_{est} \rightarrow \infty$ , and for all  $c > 0$*

$$\sup_{\substack{s \in \mathcal{S}_c \\ \pi_0 \in \Pi_0}} |\widehat{\lambda}_{\pi_0}(s) - \lambda_{\pi_0}(s)| \xrightarrow{p} 0 \quad (32)$$

as  $n_{est} \rightarrow \infty$ , and that  $\mathbb{E}_{\mathbf{S}}(T_w(A))$  is a continuous function of  $A$ . Then for given  $A$ , for all  $\eta > 0$  we have

$$P_{\mathbf{S}^*} \left( |\mathbb{E}_{\mathbf{S}^*}(\widetilde{T}_w(A)) - \mathbb{E}_{\mathbf{S}}(T_w(A))| < \eta \right) \rightarrow 1 \quad (33)$$

as  $n_{est} \rightarrow \infty$ .

*Proof.* See Appendix A.3. □

From Lai (1998), we know that  $T_w(A)$  is first-order optimal as  $A \rightarrow \infty$ . Theorem 2 tells us that for any threshold  $A$ , the operating characteristics of  $\widetilde{T}_w(A)$  converge to the operating characteristics of  $T_w(A)$  as  $n_{est} \rightarrow \infty$ .

An alternative to mixing over  $\Pi_0$  is to maximize over possible values of  $\pi_0$  at each time step. This is the generalized likelihood ratio (GLR) approach, and has also been studied in previous research (see, e.g., Siegmund and Venkatraman (1995)). For exponential families, some optimality properties of the GLR have been shown, but it is typically harder to control the average run length to false alarm (Tartakovsky et al., 2014).

### 2.3 Density estimates and least favorable pairs for $\pi_\infty$ and $\pi_0$

A potential drawback of the mixture approach is that computing or approximating the integrals in (28) may be computationally intensive. One alternative is to address the uncertainty in the pre- and post-change mixing parameters by considering worst-case performance. This was initially developed by Unnikrishnan et al. (2011); we apply their approach to unknown  $\pi_\infty$  and  $\pi_0$ . The same approach can also be used when  $\pi_\infty$  is known, as above, but we will address the more general case here.

Suppose that  $\pi_\infty \in \Pi_\infty$  and  $\pi_0 \in \Pi_0$ , where  $\Pi_\infty$  and  $\Pi_0$  are disjoint closed subintervals of  $[0, 1]$ . Separation between  $\Pi_\infty$  and  $\Pi_0$  is the price we pay for unknown  $\pi_\infty$  or  $\pi_0$ . Furthermore, if  $\Pi_\infty$  and  $\Pi_0$  are disjoint closed subintervals, then all elements of one set are greater than all elements of the other. This ordering is important for determining worst-case performance. We begin by describing the procedure when  $f_\infty^1$  and  $f_\infty^0$  are known, then consider the modification that uses density estimates  $\hat{f}_\infty^1$  and  $\hat{f}_\infty^0$ .

The true densities  $f_\infty$  and  $f_0$  are given by (5), but  $\pi_\infty$  and  $\pi_0$  are unknown. Instead, consider fixed  $\pi'_\infty \in \Pi_\infty$  and  $\pi'_0 \in \Pi_0$ , corresponding to the densities

$$\begin{aligned} g_\infty(s) &= \pi'_\infty f_\infty^1(s) + (1 - \pi'_\infty) f_\infty^0(s) \\ g_0(s) &= \pi'_0 f_0^1(s) + (1 - \pi'_0) f_0^0(s), \end{aligned} \quad (34)$$

and the detection procedure

$$T_{\pi'_\infty, \pi'_0}(A) = \inf \left\{ t \geq 1 : \max_{1 \leq k \leq t} \prod_{i=k}^t \frac{g_0(S_i)}{g_\infty(S_i)} \geq A \right\}. \quad (35)$$

Since  $\pi'_\infty$  and  $\pi'_0$  may not be the true  $\pi_\infty$  and  $\pi_0$ , we need to consider the performance of  $T_{\pi'_\infty, \pi'_0}(A)$  under the true parameters. Let  $\mathbb{E}_\nu^{\pi_\infty, \pi_0}$  denote expectation when the changepoint is  $\nu$  and the pre- and post-change parameters are  $\pi_\infty$  and  $\pi_0$ . We choose  $\pi'_\infty \in \Pi_\infty$  and  $\pi'_0 \in \Pi_0$  to maintain control on the false alarm rate while giving the worst-case detection delay. Following Unnikrishnan et al. (2011), this is formally stated as: choose  $\pi'_\infty$  and  $\pi'_0$  such that

$$\begin{aligned} \inf_{(\pi_\infty, \pi_0) \in \Pi_\infty \times \Pi_0} \mathbb{E}_\infty^{\pi_\infty, \pi_0}(T_{\pi'_\infty, \pi'_0}(A)) &\geq \mathbb{E}_\infty^{\pi'_\infty, \pi'_0}(T_{\pi'_\infty, \pi'_0}(A)) \\ \sup_{\substack{(\pi_\infty, \pi_0) \in \Pi_\infty \times \Pi_0 \\ 0 \leq \nu < \infty}} \{ \text{ess sup} \mathbb{E}_\nu^{\pi_\infty, \pi_0}[(T_{\pi'_\infty, \pi'_0}(A) - \nu)^+ | S_1, \dots, S_\nu] \} &= \sup_{0 \leq \nu < \infty} \{ \text{ess sup} \mathbb{E}_\nu^{\pi'_\infty, \pi'_0}[(T_{\pi'_\infty, \pi'_0}(A) - \nu)^+ | S_1, \dots, S_\nu] \} \\ &\leq \sup_{\substack{(\pi_\infty, \pi_0) \in \Pi_\infty \times \Pi_0 \\ 0 \leq \nu < \infty}} \{ \text{ess sup} \mathbb{E}_\nu^{\pi_\infty, \pi_0}[(T - \nu)^+ | S_1, \dots, S_\nu] \}, \end{aligned} \quad (36)$$

where  $T$  is any stopping time with  $\inf_{(\pi_\infty, \pi_0) \in \Pi_\infty \times \Pi_0} \mathbb{E}_\infty^{\pi_\infty, \pi_0}(T) \geq \mathbb{E}_\infty^{\pi'_\infty, \pi'_0}(T_{\pi'_\infty, \pi'_0}(A))$ . If  $\pi'_\infty, \pi'_0$  satisfy (36), then the resulting pair  $(g_\infty, g_0)$  is called the *least favorable pair* for  $\Pi_\infty \times \Pi_0$ . Intuitively, the worst-case is given when  $\pi'_\infty$  and  $\pi'_0$  are as close as possible, as this makes it hardest to distinguish between the pre- and post-change distributions. The following corollary applies the results in Unnikrishnan et al. (2011) to the label shift case, to show that a least favorable pair can be found and that the least favorable pair comes from minimizing  $|\pi'_0 - \pi'_\infty|$ .

**Corollary 1.** Choose  $\pi'_\infty$  and  $\pi'_0$  as follows:

- (a) If  $\max \Pi_\infty < \min \Pi_0$ , let  $\pi'_\infty = \max \Pi_\infty$  and  $\pi'_0 = \min \Pi_0$
- (b) If  $\max \Pi_0 < \min \Pi_\infty$ , let  $\pi'_\infty = \min \Pi_\infty$  and  $\pi'_0 = \max \Pi_0$

and suppose that  $\log(g_0(s)/g_\infty(s))$  is continuous over the support of  $g_\infty$ , and  $P_\infty(Y_i = 1|S_i = s)$  is an increasing function of  $s$ . Then  $(g_\infty, g_0)$  is a least favorable pair for  $\Pi_\infty \times \Pi_0$ .

*Proof.* See Appendix A.4.  $\square$

The above result requires known conditional densities. The intuition is that replacing these with conditional density estimates  $\hat{f}_\infty^1$  and  $\hat{f}_\infty^0$  should produce an approximately least-favorable pair  $(\hat{g}_\infty, \hat{g}_0)$ :

$$\begin{aligned}\hat{g}_\infty(s) &= \pi'_\infty \hat{f}_\infty^1(s) + (1 - \pi'_\infty) \hat{f}_\infty^0(s) \\ \hat{g}_0(s) &= \pi'_0 \hat{f}_\infty^1(s) + (1 - \pi'_0) \hat{f}_\infty^0(s),\end{aligned}\tag{37}$$

and the estimated least-favorable stopping rule:

$$\tilde{T}_{\pi'_\infty, \pi'_0}(A) = \inf \left\{ t \geq 1 : \max_{1 \leq k \leq t} \prod_{i=k}^t \frac{\hat{g}_0(S_i)}{\hat{g}_\infty(S_i)} \geq A \right\}.\tag{38}$$

Applying Theorem 1, we show that  $\mathbb{E}_{\mathbf{S}|\mathbf{S}^*}(\tilde{T}_{\pi'_\infty, \pi'_0}(A))$  converges in probability to  $\mathbb{E}_{\mathbf{S}}(T_{\pi'_\infty, \pi'_0}(A))$  as  $n_{est} \rightarrow \infty$ .

**Corollary 2.** Suppose that for all  $c > 0$ ,

$$\sup_{s \in \mathcal{S}_c} \left| \frac{\hat{g}_0(s)}{\hat{g}_\infty(s)} - \frac{g_0(s)}{g_\infty(s)} \right| \xrightarrow{p} 1\tag{39}$$

as  $n_{est} \rightarrow \infty$ , and that  $\mathbb{E}_{\mathbf{S}}(T_{\pi'_\infty, \pi'_0}(A))$  is a continuous function of  $A$ . Then for given  $A$ , for all  $\eta > 0$  we have

$$P_{\mathbf{S}^*} \left( |\mathbb{E}_{\mathbf{S}|\mathbf{S}^*}(\tilde{T}_{\pi'_\infty, \pi'_0}(A)) - \mathbb{E}_{\mathbf{S}}(T_{\pi'_\infty, \pi'_0}(A))| < \eta \right) \rightarrow 1\tag{40}$$

as  $n_{est} \rightarrow \infty$ .

*Proof.* The result follows directly from Theorem 1.  $\square$

When  $\hat{\lambda} = \hat{g}_0/\hat{g}_\infty$ , with  $\hat{g}_0$  and  $\hat{g}_\infty$  as in (37), the least-favorable choice of  $\pi'_\infty$  and  $\pi'_0$  minimize  $|\pi'_0 - \pi'_\infty|$ . Corollary 2 shows that the least-favorable procedure for given density estimates  $\hat{f}_\infty^1$  and  $\hat{f}_\infty^0$ , is close to the least favorable procedure when  $f_\infty^1$  and  $f_\infty^0$  are known. If  $f_\infty^1$  and  $f_\infty^0$  were known, we could estimate the operating characteristics of the least-favorable detection procedure, which would give worst-case bounds on the true operating characteristics. However, because  $\hat{f}_\infty^1$  and  $\hat{f}_\infty^0$  are not the true densities, it is hard to compute operating characteristics of the estimated least-favorable procedure. This means that, in practice, we can't compute a bound on detection delay, because we don't know the worst-case  $f_\infty^1$  and  $f_\infty^0$ .

It is tempting to address the uncertainty in the densities  $f_\infty^1$  and  $f_\infty^0$  in the same way as we did with  $\pi_\infty$  and  $\pi_0$ , by choosing worst case density estimates. Unfortunately, defining least-favorable estimates of  $f_\infty^1$  and  $f_\infty^0$  is challenging, as we discuss in Section 4.

### 3 Simulation study

In this section, we investigate the empirical performance of the label shift detection procedure in (18), and compare to other procedures from the literature. Our main simulation setting is the mixture of bivariate Gaussians described in (7), with an LDA classifier described in (8). We again choose to focus on LDA as a source of classifier scores because the explicit class score densities can be written easily in closed form

(9), allowing comparison of the performance of methods based on the estimated likelihood ratio  $\hat{\lambda}_L$  to those based on the true likelihood ratio  $\lambda$ .

We consider six parameter combinations, varying  $\pi_0 \in \{0.2, 0.5, 0.7\}$  and  $\boldsymbol{\mu}_1 \in \{[0.5, 0.5]^T, [1.5, 1.5]^T\}$ . In all cases,  $\pi_\infty = 0.4$ ,  $\boldsymbol{\mu}_0 = \mathbf{0}$ , and  $\boldsymbol{\Sigma} = \mathbf{I}$ . The value of  $\pi_0$  determines the magnitude of the change in distributions, while  $\boldsymbol{\mu}_1$  determines the difference between the positive and negative classes, and therefore the performance of the classifier. A training set  $(X'_1, Y'_1), \dots, (X'_{n_{train}}, Y'_{n_{train}}) \sim \mathbb{P}_\infty$  of size  $n_{train}$  was used to estimate  $\hat{\pi}_\infty$ ,  $\hat{\boldsymbol{\mu}}_0$ ,  $\hat{\boldsymbol{\mu}}_1$ , and  $\hat{\boldsymbol{\Sigma}}$ .

We assume throughout the simulations that both  $\pi_\infty$  and  $\pi_0$  are known for the purposes of label shift detection, to focus on the impact of density estimation. We compare a variety of approaches to the changepoint detection problem, which reflect the diversity of methods and assumptions in the literature. We give each method a short name so it can be easily referred to in text and figures. The first five approaches are based on the CUSUM procedure (13), with a substitute for the true likelihood ratio when the true ratio is unknown. Full details on each method and a summary of the main simulations can be found in Appendix A.5.

We also compare with the CPM method of Ackerman et al. (2020). Because the `cpm` package (Ross, 2015) only provides a fixed set of tuning choices for ARL, we do not include these results in this section, but describe them in Appendix A.6.

**Optimal CUSUM** As a baseline for optimal performance, the optimal CUSUM method uses the true likelihood ratio on the raw data  $X_1, X_2, \dots$ . As shown in Moustakides (1986), optimal CUSUM minimizes Lorden's detection delay (10) at the specified ARL.

**GaussianEst** Optimal CUSUM assumes known pre- and post-change densities. The simplest relaxation is that the parametric form is known (a mixture of Gaussians), but the Gaussian parameters must be estimated. GaussianEst substitutes estimates of  $\boldsymbol{\mu}_0$ ,  $\boldsymbol{\mu}_1$ , and  $\boldsymbol{\Sigma}$  in the CUSUM likelihood ratio on  $X_1, X_2, \dots$ . GaussianEst represents the best we can do when the distributions are not perfectly known.

**KDE** Our proposed KDE method utilizes the label-shift assumption, but replaces the true LDA score conditional densities  $f_\infty^1$  and  $f_\infty^0$  with nonparametric kernel density estimates (18). KDE represents a balance between leveraging the label-shift assumption and removing parametric assumptions.

**uLSIF** In contrast to KDE, the nonparametric uLSIF method (Kanamori et al., 2009) estimates the LDA score likelihood ratio directly, without using the label shift structure of the likelihood ratio. Without post-change data, uLSIF still relies on the label-shift assumption to estimate the likelihood ratio: pre-change estimation data  $(S_i^*, Y_i^*)$  can be re-sampled with weights depending on  $\pi_0$  and  $\pi_\infty$  to mimic a sample of post-change data.

**NPScore** Other nonparametric procedures replace the likelihood ratio  $\lambda$  with a function  $g$  that satisfies similar properties; in particular,  $\mathbb{E}_\infty[\log g(S_i)] < 0$  and  $\mathbb{E}_0[\log g(S_i)] > 0$ . As a representative example of such procedures, we take the function described in Tartakovsky et al. (2012b). NPScore relies on the pre- and post-change means and variances of the scores  $S_i$ , which can be approximated using the estimation data  $S_i^*$  and re-sampling as in uLSIF.

**kNN** The nonparametric kNN procedure described by Chen (2019) and Chu and Chen (2018) constructs a detection statistic based on nearest-neighbor graphs in a sliding window. This nearest-neighbors method does not use a likelihood ratio or the CUSUM method, and can be applied to either raw data  $(X_1, X_2, \dots)$  or LDA scores  $(S_1, S_2, \dots)$ .

We compare detection delays between methods at  $ARL \approx 1500$ . For optimal CUSUM, we select the thresholds so that ARL is approximately 1500 in each simulation configuration. We use the same threshold for GaussianEst, KDE, NPScore, and uLSIF. Each of these four methods has variability in their operating characteristics based on the estimation sample  $(X_1^*, Y_1^*), \dots, (X_{n_{est}}^*, Y_{n_{est}}^*)$ , so we calculate ARL and detection delay for  $n_{sims} = 50$  different estimation samples, each of size  $n_{est} = 2000$ .

We use Lorden's measure of detection delay (10) for optimal CUSUM, GaussianEst, KDE, NPScore, and uLSIF. For kNN, we chose the window length  $L = 300$  and  $k = 5$ , similar to Chu and Chen (2018). To apply kNN we used the implementation in the `gstream` package (Chen and Chu, 2019). Due to computational issues with long sequences, we set the detection threshold using `gstream` calculations, rather than estimating the ARL through simulations with pre-change data; results in Chu and Chen (2018) demonstrate the accuracy of the selected threshold. To estimate the detection delay, we simulated  $(X_1, Y_1), \dots, (X_L, Y_L) \sim \mathbb{P}_\infty$  and  $(X_{L+1}, Y_{L+1}), \dots, (X_{2L}, Y_{2L}) \sim \mathbb{P}_0$ . We limited the number of observations to  $2L$  for computational reasons, and because if a change is not detected by time  $\nu + L$ , all future windows will have only post-change data with which to detect a change. The detection procedure begins at time  $L + 1$ , using  $X_1, \dots, X_L$  as historical data. A lower bound on average detection delay was measured by averaging the stopping times  $T - L$ , where a stopping time  $T$  is recorded as  $2L$  when no change is detected by time  $2L$ . We also report the proportion of runs in which no change was detected by time  $2L$ .

Along with this main simulation setting, we conduct three additional auxiliary simulations (Section 3.2) to examine particular aspects of the procedures. The first examines performance under a different setting for  $f_\infty^1$  and  $f_\infty^0$ . The second demonstrates that the variability observed in the main simulations is a general property of changepoint procedures fit on a training set, and is not specific to the classification setting. The third demonstrates that the bias-variance trade-off that we expect to observe in classifier performance also impacts the performance of changepoint procedures that are based on classifier scores.

### 3.1 Main simulation results

Tables 1 and 2 summarize our main simulations. Table 1 shows detection delay for each method at an ARL of 1500, demonstrating that KDE, GaussianEst, NPScore, and uLSIF all perform reasonably when their ARL is close to the optimal ARL. However, the ARL and detection delay of uLSIF tend to be more variable than for the other methods, as shown in Table 2. Finally, kNN has a substantially higher detection delay, at the same ARL, than the CUSUM-based procedures, likely due to its increased flexibility and minimal assumptions. The results are similar across parameter settings, so we will focus on only one setting for further discussion:  $\mu_1 = [1.5, 1.5]^T$  and  $\pi_0 = 0.5$ .

Table 2 shows variability in operating characteristics between estimation samples. The uLSIF likelihood ratio estimate is the most variable (Figure 2) whereas the KDE estimate tends to be closer to the true likelihood ratio function. Both the KDE and GaussianEst operating characteristics tend to be close to the optimal CUSUM operating characteristics, with similar variability (Figure 2 and Table 2). It is also interesting to see that while the (ARL, Detection Delay) pairs for KDE and GaussianEst vary around the optimal CUSUM operating characteristics, at each realized ARL the detection delay is close to the optimal CUSUM detection at that ARL (Figure 2).

Theorem 1 states that the KDE operating characteristics will converge in probability to the optimal CUSUM operating characteristics as the sample size  $n_{est} \rightarrow \infty$ , and Figure 2 gives an empirical sense of the rate of convergence. KDE and GaussianEst also appear to have similar rates of convergence; since GaussianEst represents the best we can do without perfect information of the pre- and post-change distributions, our results suggest it would be difficult to improve on KDE in these simulations.

Since the LDA scores  $S_i \in [0, 1]$ , we used beta kernel density estimation (Chen, 1999) for  $\hat{f}_\infty^0$  and  $\hat{f}_\infty^1$ . To pick the bandwidths  $h$  for KDE in the lower two panels of Figure 2, we require  $h \rightarrow 0$  and  $n_{est}h^2 \rightarrow \infty$ , to ensure uniform convergence of the beta kernel density estimator (Bouezmarni and Rolin, 2003). Here we chose  $h = n_{est}^{-0.45}$ ; in general, optimal bandwidth selection for changepoint detection is a question of interest. Simulations suggest that for a fixed sample size, some under-smoothing tends to produce more reliable operating characteristics. Both approaches yield similar variability in the operating characteristics, but over-smoothing produces a bias in the operating characteristics (Figure 3).

Simulation Parameters		Detection Delay when ARL = 1500						
$\mu_1$	$\pi_0$	Optimal CUSUM	KDE	GaussianEst	NPScore	uLSIF	kNN (raw) (not detected)	kNN (LDA) (not detected)
$[0.5, 0.5]^T$	0.2	212	214	213	217	247	$\geq 267$ (0.80)	$\geq 269$ (0.81)
	0.5	458	473	458	483	NA	$\geq 273$ (0.84)	$\geq 267$ (0.82)
	0.7	133	133	131	134	146	$\geq 265$ (0.79)	$\geq 265$ (0.79)
$[1.5, 1.5]^T$	0.2	68.1	68.3	67.9	68.7	69.6	$\geq 243$ (0.67)	$\geq 243$ (0.68)
	0.5	180	180	179	183	193	$\geq 266$ (0.62)	$\geq 265$ (0.61)
	0.7	38.5	39.0	38.6	39.4	39.2	$\geq 198$ (0.44)	$\geq 204$ (0.47)

**Table 1:** We compare the approximate detection delay of each procedure at each combination of  $\mu_1$  and  $\pi_0$  in our simulations. For optimal CUSUM, KDE, GaussianEst, NPScore, and uLSIF, detection delay is measured using Lorden’s criterion (10). For kNN, we use a window size  $L = 300$  and limit the number of post-change observations to  $L$  – after a full window of post-change observations, future windows will have no pre-change observations with which to detect a change. We thus get a lower bound on detection delay, as described in Section 3, and also report in parentheses the fraction of runs in which no change was detected by the end of the post-change observations. For KDE, GaussianEst, NPScore, and uLSIF we calculate ARL and detection delay from 50 different estimation samples. Because of variability in these operating characteristics between estimation samples, to compare procedures we estimate the detection delay at ARL = 1500 by local regression smoothing on the (ARL, detection delay) pairs. The observed NA for uLSIF occurs because the (ARL, detection delay) pairs were too variable to estimate delay when ARL = 1500.

Parameters		Observed (10th, 90th) Quantiles of Operating Characteristics							
		KDE		GaussianEst		NPScore		uLSIF	
$\mu_1$	$\pi_0$	ARL	Detection Delay	ARL	Detection Delay	ARL	Detection Delay	ARL	Detection Delay
$[0.5, 0.5]^T$	0.2	(727, 2088)	(161, 247)	(773, 3118)	(161, 289)	(665, 2244)	(153, 259)	(136, 4334)	(91.1, 543)
	0.5	(1400, 5355)	(448, 988)	(800, 3846)	(306, 718)	(741, 2682)	(311, 623)	(91.8, 9291)	(74.1, 2021)
	0.7	(1088, 4136)	(117, 186)	(963, 3448)	(112, 166)	(810, 2523)	(108, 158)	(134, 8134)	(59.6, 321)
$[1.5, 1.5]^T$	0.2	(1152, 1787)	(62.9, 71.4)	(1110, 2205)	(62.0, 75.1)	(471, 1052)	(47.6, 62.2)	(606, 3806)	(53.6, 92.4)
	0.5	(1442, 2226)	(175, 209)	(1118, 1987)	(159, 198)	(706, 3345)	(131, 242)	(411, 9759)	(126, 489)
	0.7	(1400, 2227)	(38.3, 43.2)	(1228, 1957)	(36.8, 40.9)	(961, 2341)	(35.5, 43.9)	(746, 3336)	(33.3, 46.8)

**Table 2:** For procedures that require an estimation sample, we compare the 10th and 90th quantiles of operating characteristics across estimation samples. Detection delay is measured according to Lorden’s criterion (10).

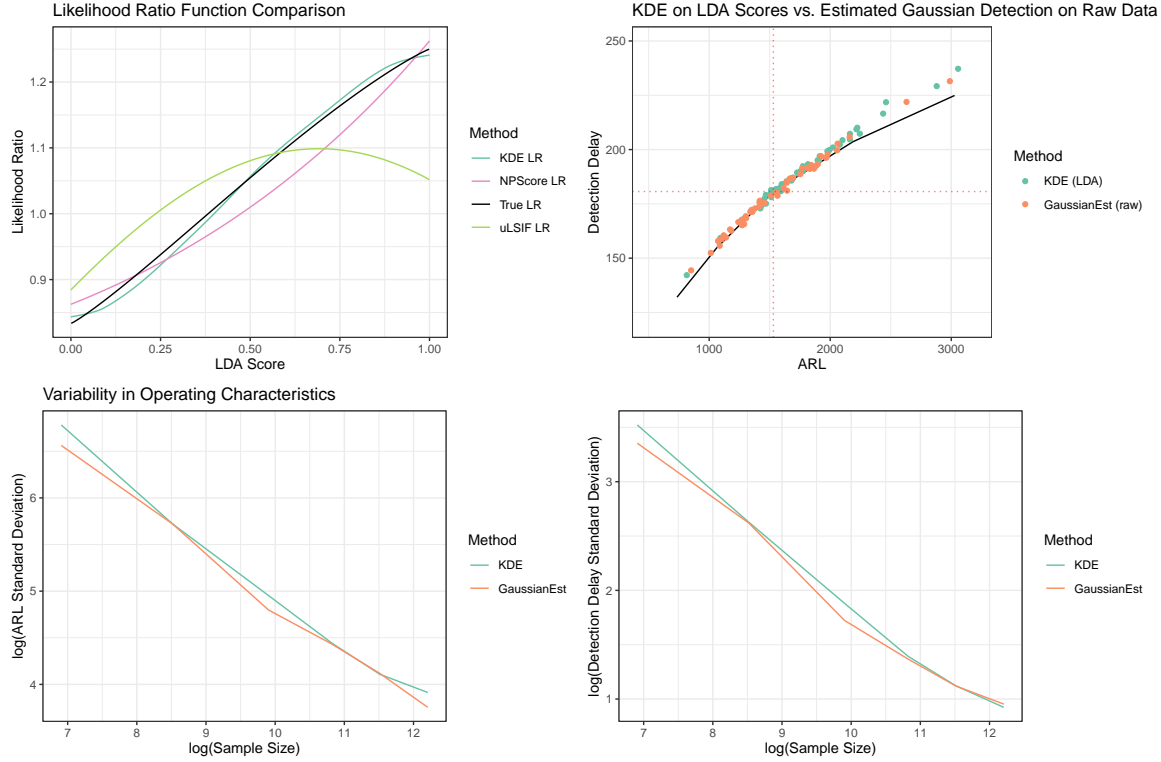


**Figure 2:** Simulation results when  $\mu_1 = [1.5, 1.5]^T$  and  $\pi_0 = 0.5$ . Top left: The true LDA score-based likelihood ratio function is shown as a black curve. Example score-based likelihood ratio functions, from one estimation sample of size 2000, are also shown for KDE, NPScore, and uLSIF. Top right: The dotted red lines show the optimal CUSUM detection delay and ARL at the threshold for which  $ARL \approx 1500$ . For KDE and GaussianEst, 50 (ARL, detection delay) pairs are plotted, each from a different estimation sample. The black curve shows the relationship between ARL and detection delay for the optimal CUSUM procedure at different thresholds. Bottom: The bottom two panels show the standard deviation of ARL (left) and detection delay (right) across estimation samples, as a function of estimation sample size  $n_{est}$ . The plots are shown on the log-log scale to better examine rates.

The strong positive relationship between ARL and detection delay, across estimation samples (Figure 2 and Figure 3), results from the likelihood ratio estimate in each sample. Figure 4 compares estimated KDE likelihood ratios between two estimation samples. In one estimation sample, the likelihood ratio is consistently overestimated, leading to shorter ARL and shorter detection delay. In the other training sample, the likelihood ratio is consistently underestimated, leading to longer ARL and longer detection delay.

### 3.2 Auxiliary simulations and results

#### 3.2.1 NPScore with different conditional distributions

We can see from Table 1 and Table 2 that NPScore does quite well in our simulations. Because NPScore replaces the likelihood ratio with a fixed function (74), its performance is determined by the suitability of that function. In this case, the function is optimal for Gaussian data, which is well-matched to the simulation likelihood ratio (Figure 2). In other settings, the NPScore will tend to have worse performance.

To investigate the performance of NPScore in other settings, we considered a label shift change where  $f_\infty^1$

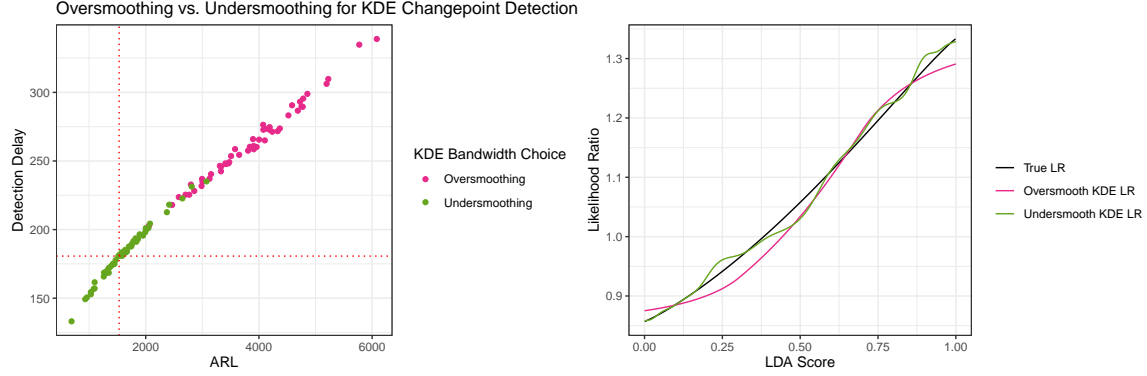


**Figure 3:** Comparison of the distribution of (ARL, detection delay) pairs for KDE with over-smoothing vs. under-smoothing. The left panel shows the distribution of operating characteristics across 50 estimation samples, with the dotted red lines showing the optimal CUSUM ARL and detection delay. The right panel shows the true likelihood ratio function as a black curve, and example KDE likelihood ratio estimates with under-smoothing and over-smoothing.

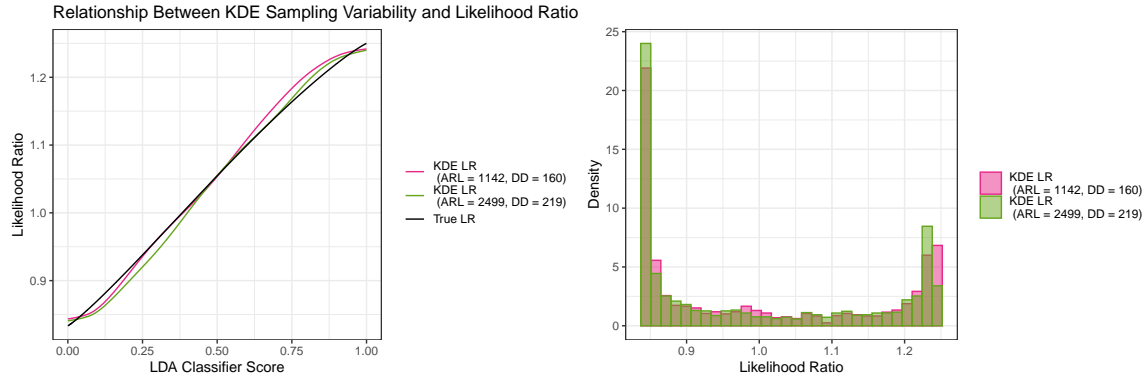


**Figure 4:** Left: The true LDA score-based likelihood ratio function is shown as a black curve. Two KDE likelihood ratio estimates are also shown, from different estimation samples. One sample led to smaller ARL and detection delay, while the other sample led to larger ARL and detection delay. Right: The pre-change distribution of likelihood ratios for the two different KDE estimates shown in the left panel. These figures provide explanation for the variability observed in the operating characteristics between estimation samples (e.g., Figure 2).

and  $f_\infty^0$  are given by

$$\begin{aligned} f_\infty^0(s) &= 64.8s(1-s)^7 + 0.2(1-s) \\ f_\infty^1(s) &= 94.5s^4(1-s)^2 + 0.2s. \end{aligned} \tag{41}$$

This is designed to compare method performance under a different likelihood ratio than the LDA likelihood ratio function. As shown in Figure 5, NPScore does noticeably worse than our KDE procedure in this setting, because the NPScore likelihood ratio is quite far from the true likelihood ratio.

### 3.2.2 Operating characteristic variability for a simple Gaussian change

In the simulation results shown above, we see variability in the operating characteristics, which results from variability in the estimation sample. In this additional simulation, we demonstrate that this variability is inherent whenever an estimation sample  $\mathbf{S}^*$  is used, and is not a result of the classification or label shift settings.

We consider a simple Gaussian change, from a  $N(0, 1)$  pre-change distribution to a  $N(1, 1)$  post-change

distribution. The pre- and post-change means and standard deviations are estimated, and we conduct changepoint detection using Gaussian densities with the estimated parameters. Figure 5 shows the result, demonstrating the same variability in ARL and detection delay that we see in Figure 2.

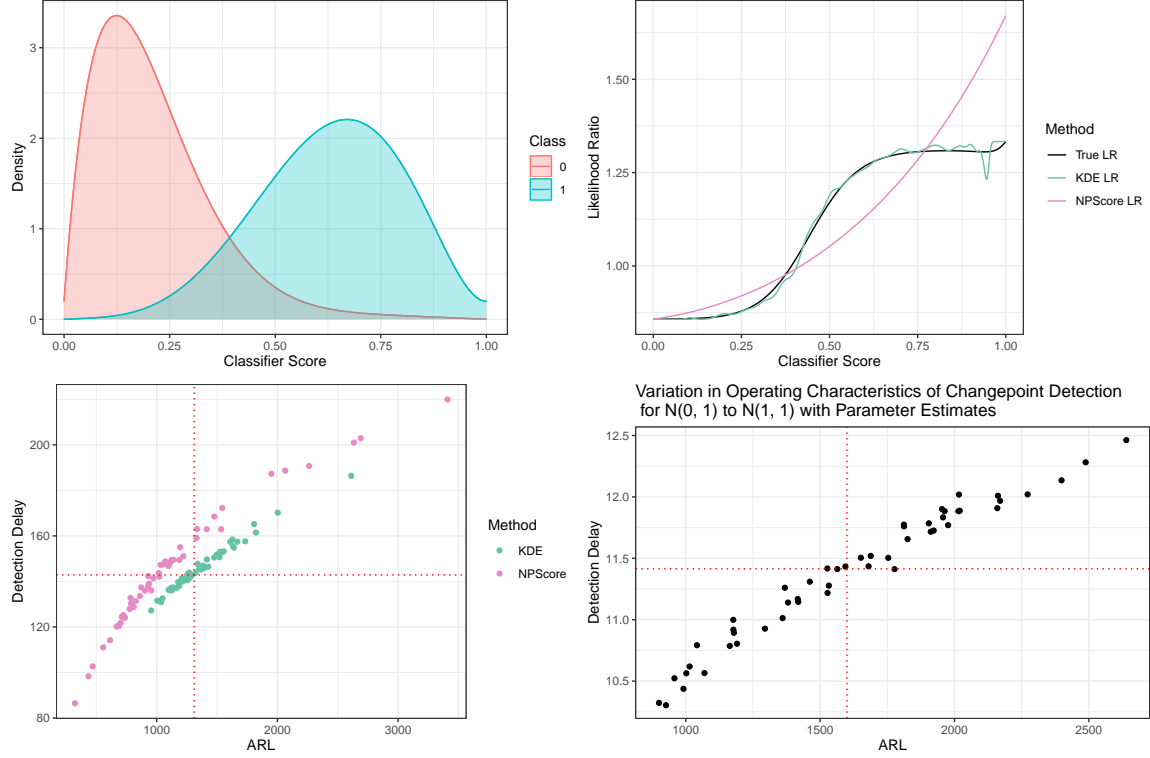


**Figure 5:** Auxiliary simulations. For contrast with the LDA simulations, we compare performance of KDE and NPScore when the conditional score densities are given by (41), with  $\pi_\infty = 0.3$  and  $\pi_0 = 0.4$ . Top left: The classifier score distributions for each class, according to (41). Top right: The true likelihood ratio function is shown as a black curve. Example likelihood ratio functions, from one estimation sample, are compared for KDE and NPScore. Bottom left: (ARL, detection delay) pairs for KDE and NPScore, from 50 different estimation samples. The dotted red lines show the optimal CUSUM detection delay and ARL (using the likelihood ratio shown as a black curve in the top right figure) at the threshold for which  $ARL \approx 1500$ . Bottom right: Our main simulation results show variability in the operating characteristics of detection procedures which require an estimation sample. For comparison, the bottom right panel examines variability of operating characteristics in a different setting: a simple univariate change from  $N(0, 1)$  to  $N(1, 1)$ . Here the pre- and post-change means, and the standard deviation, must be estimated, leading to variability depending on the estimation sample used.

### 3.2.3 Classifier performance and changepoint detection

Finally, as we discussed in Section 1.2, the performance of a detection procedure using classifier scores relies on the performance of the corresponding classifier. We demonstrate this by comparing the performance of KDE changepoint detection using either LDA or Quadratic Discriminant Analysis (QDA) scores, when the true generating distribution satisfies QDA but not LDA assumptions.

We simulate label shift data where  $X \in \mathbb{R}^{150}$ , and  $X|Y = 0 \sim N(\boldsymbol{\mu}_0, \boldsymbol{\Sigma}_0)$  and  $X|Y = 1 \sim N(\boldsymbol{\mu}_1, \boldsymbol{\Sigma}_1)$ , with  $\boldsymbol{\Sigma}_0 \neq \boldsymbol{\Sigma}_1$ . Note that this generating distribution satisfies the modeling assumptions of QDA but not those of LDA. However, when the training sample size is small, the higher dimension of the QDA model leads to overwhelming variance in the estimated parameters, and therefore poor performance as a classifier in comparison to the misspecified LDA model which requires fewer parameters.

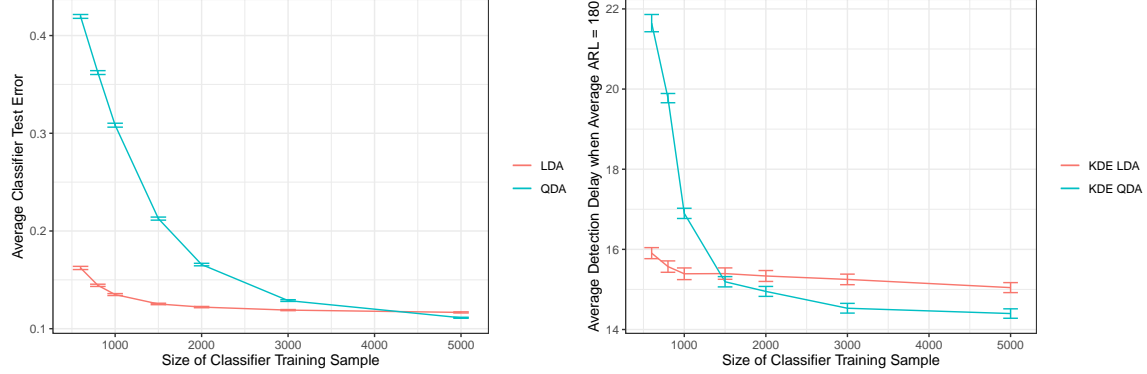


**Figure 6:** Comparison between KDE changepoint detection with LDA and QDA classifier scores, when LDA assumptions are violated but QDA assumptions are satisfied. Left: Average classifier test error on new data, as a function of the size of the classifier training sample. Right: Each LDA and QDA classifier is used for KDE changepoint detection with the classifier scores. This plot shows the average detection delay when the average ARL is approximately 180 (averaged across classifiers) as a function of the size of the classifier training sample.

Figure 6 shows the average misclassification error of these classifiers across a range of training sample sizes, along with the average detection delay for fixed average run length. Just as the relative classification error of LDA and QDA depends on the size of the training data, so does performance of a changepoint detection procedure using their scores. As we see in Figure 6, small training samples have a better detection delay using LDA scores because of their reduced estimation variance, even though the LDA model is mis-specified. At larger sample sizes where variance is less of an issue, QDA performs better for both classification and changepoint detection. This is reassuring – the same intuition about bias-variance trade-offs that drives classifier training also drives performance of the detection procedures.

## 4 Discussion

In this paper, we consider the problem of detecting label shift in sequentially observed classification data. Because classifier training inherently requires pre-change data, we can estimate the pre- and post-change distributions up to a potentially unknown scalar post-change parameter. Furthermore, we reduce the problem to changepoint detection in the univariate classifier scores, a particular advantage when the data are high dimensional or does not follow convenient parametric assumptions. We develop and study a simple procedure (14) that incorporates density estimates  $\hat{f}_\infty^1$  and  $\hat{f}_\infty^0$  into a CUSUM rule by relying on the label-shift assumption (18).

We show in Theorem 1 that the resulting nonparametric density procedure is consistent for the operating characteristics of the optimal CUSUM procedure on the classifier scores, as the estimation sample size  $n_{est} \rightarrow \infty$ . While performance of the optimal CUSUM procedure on the classifier scores depends on the classifier, even a misspecified classifier can perform well for detecting label shift (e.g., Figure 5).

We consider two generalizations to address lack of knowledge about the post-change mixing parameter  $\pi_0$ . When knowledge of  $\pi_0$  is limited, we can instead mix over possible values of  $\pi_0$  (Theorem 2) or take a worst-case  $\pi_0$  (Corollary 2). In both cases, we show that our density estimation approach is consistent. Mixing over the post-change parameter is expected to give a better detection delay than choosing the worst-case  $\pi_0$ , particularly for large ARL, but is more computationally expensive than using the least-favorable  $\pi_0$ . Furthermore, if  $f_\infty^1$  and  $f_\infty^0$  were known, the least-favorable procedure would allow us to calculate a bound on the detection delay. While we can't calculate that bound when  $f_\infty^1$  and  $f_\infty^0$  are unknown, Corollary 2 guarantees that our estimated worst-case procedure is close to the true worst-case procedure.

In addition to these theoretical results, we show good empirical performance of the nonparametric density procedure in simulations. While Theorem 1 does not provide a rate of convergence, simulations (Figure 2) demonstrate that convergence of the nonparametric density approach can be comparable to the “best-case” procedure where the parametric forms of the score distributions are known.

Our theoretical results rely on a likelihood ratio  $\lambda$  that is bounded, with an estimate  $\hat{\lambda}$  that is bounded and converges uniformly to  $\lambda$  on each set  $\mathcal{S}_c$ . Any estimate  $\hat{\lambda}$  which satisfies these requirements is suitable, but proving boundedness or convergence for a general likelihood ratio estimate is harder than for the explicit estimate  $\hat{\lambda}_L$  used in (18). By leveraging the label-shift assumption (2), our  $\hat{\lambda}_L$  guarantees the necessary bounds on the likelihood ratio.

An additional advantage of this nonparametric density approach is that mixtures over  $\pi_0$  are handled easily through the label shift structure of the likelihood ratio; methods that estimate the likelihood ratio directly, like uLSIF (Kanamori et al., 2009), do not naturally allow uncertainty in the post-change parameter. Finally, because our nonparametric density procedure is designed specifically for the label shift setting, it outperforms more flexible nonparametric change detection procedures like the nearest-neighbor approach in Chen (2019) and Chu and Chen (2018).

**Remark - least favorable distributions:** In Section 2.3, we apply the least favorable distributions (LFD) approach (Unnikrishnan et al., 2011) to address uncertainty in  $\pi_\infty$  and  $\pi_0$ , giving an upper bound on detection delay and a lower bound on ARL. In particular, we show that when density estimates  $\hat{f}_\infty^1$  and  $\hat{f}_\infty^0$  are used, the worst-case choice of  $\pi'_\infty$  and  $\pi'_0$  is still to minimize  $|\pi'_0 - \pi'_\infty|$ .

If  $f_\infty^1$  and  $f_\infty^0$  were known, the motivation for using the least-favorable  $\pi'_\infty$  and  $\pi'_0$  would be as follows: if  $\pi'_\infty, \pi'_0$  are the true parameter values, we can estimate the operating characteristics of the changepoint detection procedure. If  $\pi'_\infty$  and  $\pi'_0$  are NOT the true parameter values, these estimated operating characteristics are still guaranteed worst-case bounds.

When  $f_\infty^1$  and  $f_\infty^0$  are unknown, we may wish to obtain stronger bounds than in Section 2.3 by considering a worst case pair of *densities*  $\hat{f}_\infty^1, \hat{f}_\infty^0$ . Unfortunately, we cannot similarly define such a pair in a principled way. Let  $\mathcal{F}_\infty^1$  and  $\mathcal{F}_\infty^0$  be sets of possible distributions  $F_\infty^1$  and  $F_\infty^0$  for  $S_i|Y_i = 1$  and  $S_i|Y_i = 0$  respectively, with densities  $f_\infty^1$  and  $f_\infty^0$ . In Section 2.3 we were able to select parameters  $\pi'_\infty$  and  $\pi'_0$  for the pre- and post-change distributions independently, but any uncertainty in the conditional densities impacts both the pre- and post-change densities because of the label-shift assumption. Define

$$\mathcal{F} = \{(F_\infty, F_0) : F_\infty = \pi_\infty F_\infty^1 + (1 - \pi_\infty) F_\infty^0, \quad F_0 = \pi_0 F_\infty^1 + (1 - \pi_0) F_\infty^0, \quad (F_\infty^1, F_\infty^0) \in \mathcal{F}_\infty^1 \times \mathcal{F}_\infty^0\}. \quad (42)$$

Following the discussion in Appendix A.4,  $(\hat{f}_\infty^1, \hat{f}_\infty^0)$  are a least-favorable pair, with associated distribution functions  $(\tilde{F}_\infty, \tilde{F}_0) \in \mathcal{F}$ , if for any  $(F_\infty, F_0) \in \mathcal{F}$  we have  $F_\infty(s) \leq \tilde{F}_\infty(s)$  and  $F_0(s) \geq \tilde{F}_0(s)$  for all  $s$ .

This implies that, for all  $s$ ,

$$\begin{aligned} \pi_\infty(\tilde{F}_\infty^1(s) - F_\infty^1(s)) &\geq (1 - \pi_\infty)(F_\infty^0(s) - \tilde{F}_\infty^0(s)) \\ \pi_0(\tilde{F}_\infty^1(s) - F_\infty^1(s)) &\leq (1 - \pi_0)(F_\infty^0(s) - \tilde{F}_\infty^0(s)), \end{aligned} \quad (43)$$

which is impossible.

**Remark - mixtures:** While this manuscript focuses on the setting of binary classification with label shift, our results would extend to detecting changes in the mixing parameters of a mixture distribution, provided that the component distributions can be estimated well. If labeled data were available for each component, the methods in the paper would clearly apply directly. Even when component labels are unavailable, our results could be applied to the estimated component distributions, such as the EM algorithm of parametric mixtures. Guarantees about the reliability of those component estimates would be desirable, e.g. those provided by Balakrishnan et al. (2017).

## Acknowledgments

We thank Samuel Ackerman, Chris Genovese, Aaditya Ramdas, Alessandro Rinaldo, and Zack Lipton for helpful discussions and feedback. Both authors received partial support from NSF DMS1613202.

## References

Ackerman, S., Dube, P., and Farchi, E. (2020). Sequential drift detection in deep learning classifiers. *arXiv preprint arXiv:2007.16109*.

Azizzadenesheli, K., Liu, A., Yang, F., and Anandkumar, A. (2019). Regularized learning for domain adaptation under label shifts. *arXiv preprint arXiv:1903.09734*.

Balakrishnan, S., Wainwright, M. J., Yu, B., et al. (2017). Statistical guarantees for the EM algorithm: From population to sample-based analysis. *The Annals of Statistics*, 45(1):77–120.

Baron, M. I. (2000). Nonparametric adaptive change point estimation and on line detection. *Sequential Analysis*, 19(1-2):1–23.

Bell, C., Gordon, L., and Pollak, M. (1994). An efficient nonparametric detection scheme and its application to surveillance of a bernoulli process with unknown baseline. *Lecture Notes-Monograph Series*, pages 7–27.

Bouezmarni, T. and Rolin, J.-M. (2003). Consistency of the beta kernel density function estimator. *The Canadian Journal of Statistics/La Revue Canadienne de Statistique*, pages 89–98.

Brodsky, E. and Darkhovsky, B. S. (1993). *Nonparametric methods in change point problems*, volume 243. Springer Science & Business Media.

Brodsky, E. and Darkhovsky, B. S. (2000). *Non-parametric statistical diagnosis: problems and methods*, volume 509. Springer Science & Business Media.

Chen, H. (2019). Sequential change-point detection based on nearest neighbors. *The Annals of Statistics*, 47(3):1381–1407.

Chen, H. and Chu, L. (2019). *gStream: Graph-Based Sequential Change-Point Detection for Streaming Data*. R package version 0.2.0.

Chen, S. X. (1999). Beta kernel estimators for density functions. *Computational Statistics & Data Analysis*, 31(2):131–145.

Chu, L. and Chen, H. (2018). Sequential change-point detection for high-dimensional and non-euclidean data. *arXiv preprint arXiv:1810.05973*.

Giné, E. and Guillou, A. (2002). Rates of strong uniform consistency for multivariate kernel density estimators. In *Annales de l’Institut Henri Poincaré (B) Probability and Statistics*, volume 38, pages 907–921. Elsevier.

Gordon, L. and Pollak, M. (1994). An efficient sequential nonparametric scheme for detecting a change of distribution. *The Annals of Statistics*, pages 763–804.

Gordon, L. and Pollak, M. (1995). A robust surveillance scheme for stochastically ordered alternatives. *The Annals of Statistics*, pages 1350–1375.

Gretton, A., Smola, A., Huang, J., Schmittfull, M., Borgwardt, K., and Schölkopf, B. (2009). Covariate shift by kernel mean matching. *Dataset shift in machine learning*, 3(4):5.

Hawkins, D. M., Qiu, P., and Kang, C. W. (2003). The changepoint model for statistical process control. *Journal of quality technology*, 35(4):355–366.

Kanamori, T., Hido, S., and Sugiyama, M. (2009). A least-squares approach to direct importance estimation. *Journal of Machine Learning Research*, 10(Jul):1391–1445.

Kawahara, Y. and Sugiyama, M. (2009). Change-point detection in time-series data by direct density-ratio estimation. In *Proceedings of the 2009 SIAM International Conference on Data Mining*, pages 389–400. SIAM.

Lai, T. L. (1998). Information bounds and quick detection of parameter changes in stochastic systems. *IEEE Transactions on Information Theory*, 44(7):2917–2929.

Lipton, Z. C., Wang, Y.-X., and Smola, A. (2018). Detecting and correcting for label shift with black box predictors. *arXiv preprint arXiv:1802.03916*.

Liu, S., Yamada, M., Collier, N., and Sugiyama, M. (2013). Change-point detection in time-series data by relative density-ratio estimation. *Neural Networks*, 43:72–83.

Lorden, G. (1971). Procedures for reacting to a change in distribution. *The Annals of Mathematical Statistics*, 42(6):1897–1908.

Madrid Padilla, O. H., Athey, A., Reinhart, A., and Scott, J. G. (2019). Sequential nonparametric tests for a change in distribution: an application to detecting radiological anomalies. *Journal of the American Statistical Association*, 114(526):514–528.

Makiyama, K. (2019). *densratio: Density Ratio Estimation*. R package version 0.2.1.

McDonald, D. (1990). A CUSUM procedure based on sequential ranks. *Naval Research Logistics*, 37(5):627–646.

Mei, Y. (2006). Sequential change-point detection when unknown parameters are present in the pre-change distribution. *The Annals of Statistics*, 34(1):92–122.

Moss, J. and Tveten, M. (2019). *kdensity: Kernel Density Estimation with Parametric Starts and Asymmetric Kernels*. R package version 1.0.1.

Moustakides, G. V. (1986). Optimal stopping times for detecting changes in distributions. *The Annals of Statistics*, 14(4):1379–1387.

Page, E. S. (1954). Continuous inspection schemes. *Biometrika*, 41(1/2):100–115.

Pollak, M. (1985). Optimal detection of a change in distribution. *The Annals of Statistics*, pages 206–227.

R Core Team (2020). *R: A Language and Environment for Statistical Computing*. R Foundation for Statistical Computing, Vienna, Austria.

Rabanser, S., Günemann, S., and Lipton, Z. (2019). Failing loudly: An empirical study of methods for detecting dataset shift. *Advances in Neural Information Processing Systems* 32.

Roberts, S. (1966). A comparison of some control chart procedures. *Technometrics*, 8(3):411–430.

Ross, G. J. (2015). Parametric and nonparametric sequential change detection in R: The cpm package. *Journal of Statistical Software*, 66(3):1–20.

Ross, G. J. and Adams, N. M. (2012). Two nonparametric control charts for detecting arbitrary distribution changes. *Journal of Quality Technology*, 44(2):102–116.

Saerens, M., Latinne, P., and Decaestecker, C. (2002). Adjusting the outputs of a classifier to new a priori probabilities: a simple procedure. *Neural computation*, 14(1):21–41.

Shimodaira, H. (2000). Improving predictive inference under covariate shift by weighting the log-likelihood function. *Journal of statistical planning and inference*, 90(2):227–244.

Shiryayev, A. N. (2007). *Optimal stopping rules*, volume 8. Springer Science & Business Media.

Siegmund, D. and Venkatraman, E. (1995). Using the generalized likelihood ratio statistic for sequential detection of a change-point. *The Annals of Statistics*, pages 255–271.

Storkey, A. (2009). When training and test sets are different: characterizing learning transfer. *Dataset shift in machine learning*, pages 3–28.

Sugiyama, M., Suzuki, T., Nakajima, S., Kashima, H., von Bünau, P., and Kawanabe, M. (2008). Direct importance estimation for covariate shift adaptation. *Annals of the Institute of Statistical Mathematics*, 60(4):699–746.

Tange, O. (2011). GNU parallel—the command-line power tool. *The USENIX Magazine*, 36(1):42–47.

Tartakovsky, A., Nikiforov, I., and Basseville, M. (2014). *Sequential analysis: Hypothesis testing and change-point detection*. Chapman and Hall/CRC.

Tartakovsky, A. G., Pollak, M., and Polunchenko, A. S. (2012a). Third-order asymptotic optimality of the generalized shiryayev–roberts changepoint detection procedures. *Theory of Probability & Its Applications*, 56(3):457–484.

Tartakovsky, A. G., Polunchenko, A. S., and Sokolov, G. (2012b). Efficient computer network anomaly detection by changepoint detection methods. *IEEE Journal of Selected Topics in Signal Processing*, 7(1):4–11.

Tartakovsky, A. G., Rozovskii, B. L., Blažek, R. B., and Kim, H. (2006a). Detection of intrusions in information systems by sequential change-point methods. *Statistical methodology*, 3(3):252–293.

Tartakovsky, A. G., Rozovskii, B. L., Blazek, R. B., and Kim, H. (2006b). A novel approach to detection of intrusions in computer networks via adaptive sequential and batch-sequential change-point detection methods. *IEEE transactions on signal processing*, 54(9):3372–3382.

Unnikrishnan, J., Veeravalli, V. V., and Meyn, S. P. (2011). Minimax robust quickest change detection. *IEEE Transactions on Information Theory*, 57(3):1604–1614.

## A Appendix

### A.1 Proof of Lemma 1

*Proof.* Let  $\delta > 0$ . We want to show that  $P_{\mathbf{S}^*} \left( \sup_{s \in \mathcal{S}_c} |\widehat{\lambda}_L(s) - \lambda(s)| < \delta \right) \rightarrow 1$ . Since the conditional densities and parameter estimates converge, then

$$\sup_{s \in \mathcal{S}_c} |\widehat{f}_0(s) - f_0(s)| \xrightarrow{p} 0 \quad \sup_{s \in \mathcal{S}_c} |\widehat{f}_\infty(s) - f_\infty(s)| \xrightarrow{p} 0$$

where

$$\begin{aligned} f_\infty(s) &= \pi_\infty f_\infty^1(s) + (1 - \pi_\infty) f_\infty^0(s) & \widehat{f}_\infty(s) &= \widehat{\pi}_\infty \widehat{f}_\infty^1(s) + (1 - \widehat{\pi}_\infty) \widehat{f}_\infty^0(s) \\ f_0(s) &= \pi_0 f_\infty^1(s) + (1 - \pi_0) f_\infty^0(s) & \widehat{f}_0(s) &= \widehat{\pi}_0 \widehat{f}_\infty^1(s) + (1 - \widehat{\pi}_0) \widehat{f}_\infty^0(s). \end{aligned} \tag{44}$$

Next,

$$\begin{aligned} \left| \frac{\widehat{f}_0(s)}{\widehat{f}_\infty(s)} - \frac{f_0(s)}{f_\infty(s)} \right| &\leq \left| \frac{\widehat{f}_0(s)}{\widehat{f}_\infty(s)} - \frac{f_0(s)}{\widehat{f}_\infty(s)} \right| + \left| \frac{f_0(s)}{\widehat{f}_\infty(s)} - \frac{f_0(s)}{f_\infty(s)} \right| \\ &\leq \frac{1}{\widehat{f}_\infty(s)} |\widehat{f}_0(s) - f_0(s)| + f_0(s) \left| \frac{1}{\widehat{f}_\infty(s)} - \frac{1}{f_\infty(s)} \right|. \end{aligned} \tag{45}$$

On  $\mathcal{S}_c$ , and under the assumptions of the lemma, the right hand side converges to 0, which completes the proof.  $\square$

## A.2 Proof of Theorem 1

For ease of notation, we will drop the subscript  $CS$ .

*Proof.* The difficulty with  $\tilde{T}(A)$  and  $T(A)$  is that in theory, they have no upper bound. So to prove the result, we need to restrict ourselves to the first  $t_0$  samples,  $S_1, \dots, S_{t_0}$ , over which the behaviors of  $\tilde{R}_t$  and  $R_t$  are more manageable. Let  $U_t(A) = \min\{T(A), t\}$  and  $\tilde{U}_t(A) = \min\{\tilde{T}(A), t\}$ . To show that  $\tilde{T}(A)$  is close to  $T(A)$  in expectation, we can show that  $U_{t_0}(A)$  is close to  $\tilde{U}_{t_0}(A)$  in expectation, for sufficiently large  $t_0$ . We write

$$|\mathbb{E}_{\mathbf{S}|\mathbf{S}^*}(\tilde{T}(A)) - \mathbb{E}_{\mathbf{S}}(T(A))| \leq |\mathbb{E}_{\mathbf{S}|\mathbf{S}^*}(\tilde{T}(A)) - \mathbb{E}_{\mathbf{S}|\mathbf{S}^*}(\tilde{U}_{t_0}(A))| + |\mathbb{E}_{\mathbf{S}|\mathbf{S}^*}(\tilde{U}_{t_0}(A)) - \mathbb{E}_{\mathbf{S}}(U_{t_0}(A))| + |\mathbb{E}_{\mathbf{S}}(U_{t_0}(A)) - \mathbb{E}_{\mathbf{S}}(T(A))|. \quad (46)$$

Then we want to control each piece on the right hand side. The third term is straightforward since

$$\mathbb{E}_{\mathbf{S}}(T(A)\mathbb{I}\{T(A) \leq t\}) \leq \mathbb{E}_{\mathbf{S}}(U_t(A)) \leq \mathbb{E}_{\mathbf{S}}(T(A)), \quad (47)$$

and  $\mathbb{E}_{\mathbf{S}}(T(A)\mathbb{I}\{T(A) \leq t\}) \rightarrow \mathbb{E}_{\mathbf{S}}(T(A))$ , so  $\mathbb{E}_{\mathbf{S}}(U_t(A)) \rightarrow \mathbb{E}_{\mathbf{S}}(T(A))$  as  $t \rightarrow \infty$ .

While it is also true that for each  $\mathbf{S}^*$ ,  $\mathbb{E}_{\mathbf{S}|\mathbf{S}^*}(\tilde{U}_t(A)) \rightarrow \mathbb{E}_{\mathbf{S}|\mathbf{S}^*}(\tilde{T}(A))$  as  $t \rightarrow \infty$ , we need the convergence to happen uniformly in  $\mathbf{S}^*$  to choose an appropriate  $t_0$ .

To show that  $|\mathbb{E}_{\mathbf{S}|\mathbf{S}^*}(\tilde{U}_{t_0}(A)) - \mathbb{E}_{\mathbf{S}}(U_{t_0}(A))|$  is small, we need  $\tilde{R}_t$  close to  $R_t$  up to time  $t_0$ . Let

$$\mathcal{C}_{t_0, \varepsilon}^{\mathbf{S}^*} = \{\mathbf{S} : \sup_{t \leq t_0} |\tilde{R}_t - R_t| < \varepsilon \mid \mathbf{S}^*\}. \quad (48)$$

Then

$$|\mathbb{E}_{\mathbf{S}|\mathbf{S}^*}(\tilde{U}_{t_0}(A)) - \mathbb{E}_{\mathbf{S}}(U_{t_0}(A))| \leq |\mathbb{E}_{\mathbf{S}|\mathbf{S}^*}(\tilde{U}_{t_0}(A)) - \mathbb{E}_{\mathbf{S}|\mathbf{S}^*}(\tilde{U}_{t_0}(A)|\mathcal{C}_{t_0, \varepsilon}^{\mathbf{S}^*})| + |\mathbb{E}_{\mathbf{S}|\mathbf{S}^*}(\tilde{U}_{t_0}(A)|\mathcal{C}_{t_0, \varepsilon}^{\mathbf{S}^*}) - \mathbb{E}_{\mathbf{S}}(U_{t_0}(A))|. \quad (49)$$

If  $\mathbf{S} \in \mathcal{C}_{t_0, \varepsilon}^{\mathbf{S}^*}$ , then

$$R_t \geq A + \varepsilon \implies \tilde{R}_t \geq A \implies R_t \geq A - \varepsilon \quad t = 1, \dots, t_0, \quad (50)$$

so  $U_{t_0}(A - \varepsilon) \leq \tilde{U}_{t_0}(A) \leq U_{t_0}(A + \varepsilon)$ . And since we always have  $U_{t_0}(A - \varepsilon) \leq U_{t_0}(A) \leq U_{t_0}(A + \varepsilon)$ , then

$$\begin{aligned} |\mathbb{E}_{\mathbf{S}|\mathbf{S}^*}(\tilde{U}_{t_0}(A)|\mathcal{C}_{t_0, \varepsilon}^{\mathbf{S}^*}) - \mathbb{E}_{\mathbf{S}}(U_{t_0}(A))| &\leq |\mathbb{E}_{\mathbf{S}}(U_{t_0}(A + \varepsilon)) - \mathbb{E}_{\mathbf{S}}(U_{t_0}(A - \varepsilon))| \\ &\leq |\mathbb{E}_{\mathbf{S}}(U_{t_0}(A + \varepsilon)) - \mathbb{E}_{\mathbf{S}}(T(A + \varepsilon))| \\ &\quad + |\mathbb{E}_{\mathbf{S}}(T(A + \varepsilon)) - \mathbb{E}_{\mathbf{S}}(T(A - \varepsilon))| \\ &\quad + |\mathbb{E}_{\mathbf{S}}(U_{t_0}(A - \varepsilon)) - \mathbb{E}_{\mathbf{S}}(T(A - \varepsilon))|. \end{aligned} \quad (51)$$

Furthermore,

$$|\mathbb{E}_{\mathbf{S}|\mathbf{S}^*}(\tilde{U}_{t_0}(A)) - \mathbb{E}_{\mathbf{S}|\mathbf{S}^*}(\tilde{U}_{t_0}(A)|\mathcal{C}_{t_0, \varepsilon}^{\mathbf{S}^*})| \leq 2t_0 \left(1 - P_{\mathbf{S}|\mathbf{S}^*}(\mathcal{C}_{t_0, \varepsilon}^{\mathbf{S}^*})\right). \quad (52)$$

Thus we have

$$\begin{aligned}
|\mathbb{E}_{\mathbf{S}|\mathbf{S}^*}(\tilde{T}(A)) - \mathbb{E}_{\mathbf{S}}(T(A))| &\leq |\mathbb{E}_{\mathbf{S}|\mathbf{S}^*}(\tilde{T}(A)) - \mathbb{E}_{\mathbf{S}|\mathbf{S}^*}(\tilde{U}_{t_0}(A))| + |\mathbb{E}_{\mathbf{S}}(U_{t_0}(A)) - \mathbb{E}_{\mathbf{S}}(T(A))| \\
&\quad + 2t_0 \left(1 - P_{\mathbf{S}|\mathbf{S}^*}(\mathcal{C}_{t_0, \varepsilon}^{\mathbf{S}^*})\right) + |\mathbb{E}_{\mathbf{S}}(U_{t_0}(A + \varepsilon)) - \mathbb{E}_{\mathbf{S}}(T(A + \varepsilon))| \\
&\quad + |\mathbb{E}_{\mathbf{S}}(T(A + \varepsilon)) - \mathbb{E}_{\mathbf{S}}(T(A - \varepsilon))| \\
&\quad + |\mathbb{E}_{\mathbf{S}}(U_{t_0}(A - \varepsilon)) - \mathbb{E}_{\mathbf{S}}(T(A - \varepsilon))|.
\end{aligned} \tag{53}$$

Let  $\eta > 0$ . Since  $\mathbb{E}_{\mathbf{S}}(T(A))$  is a continuous function of  $A$ , choose  $\varepsilon > 0$  small enough that

$$|\mathbb{E}_{\mathbf{S}}(T(A + \varepsilon)) - \mathbb{E}_{\mathbf{S}}(T(A - \varepsilon))| < \eta/6. \tag{54}$$

Next, let  $c_1 > 0$  and  $0 < \delta_1 < l_\lambda$ . Define  $\lambda_{\min}$  by

$$\lambda_{\min}(s) = \begin{cases} \lambda(s) - \delta_1 & s \in \mathcal{S}_{c_1} \\ l_\lambda & s \notin \mathcal{S}_{c_1} \end{cases}. \tag{55}$$

Then if  $\sup_{s \in \mathcal{S}_{c_1}} |\hat{\lambda}(s) - \lambda(s)| < \delta_1$  and  $l_\lambda \leq \hat{\lambda}(s)$  for all  $s$ , we have  $\lambda_{\min}(s) \leq \hat{\lambda}(s)$  for all  $s \in \mathbb{R}$ . Define  $T^{\min}(A)$  by substituting  $\lambda_{\min}$  for  $\hat{\lambda}$ , so  $T^{\min}(A) \geq \tilde{T}(A)$ . Note that  $c_1$  and  $\delta_1$  are chosen sufficiently small that  $\mathbb{E}_{\mathbf{S}}(T^{\min}(A))$  is finite. Thus if  $l_\lambda \leq \hat{\lambda}(s)$  for all  $s$ , and  $\sup_{s \in \mathcal{S}_{c_1}} |\hat{\lambda}(s) - \lambda(s)| < \delta_1$ , we have

$$|\mathbb{E}_{\mathbf{S}|\mathbf{S}^*}(\tilde{T}(A)) - \mathbb{E}_{\mathbf{S}|\mathbf{S}^*}(\tilde{U}_{t_0}(A))| \leq |\mathbb{E}_{\mathbf{S}}(T^{\min}(A)) - \mathbb{E}_{\mathbf{S}}(U_{t_0}^{\min}(A))|, \tag{56}$$

because  $T^{\min}(A) \geq \tilde{T}(A)$  implies that

$$\begin{aligned}
\mathbb{E}_{\mathbf{S}|\mathbf{S}^*}(\tilde{T}(A) - \tilde{U}_{t_0}(A)) &= \mathbb{E}_{\mathbf{S}|\mathbf{S}^*}(\tilde{T}(A) - t_0 | \tilde{T}(A) > t_0) P_{\mathbf{S}|\mathbf{S}^*}(\tilde{T}(A) > t_0) \\
&\leq \mathbb{E}_{\mathbf{S}}(T^{\min}(A) - t_0 | \tilde{T}^{\min}(A) > t_0) P_{\mathbf{S}}(T^{\min}(A) > t_0) \\
&= \mathbb{E}_{\mathbf{S}}(T^{\min}(A) - U_{t_0}^{\min}(A)).
\end{aligned} \tag{57}$$

Now choose  $t_0$  sufficiently large that

$$\begin{aligned}
|\mathbb{E}_{\mathbf{S}}(T^{\min}(A)) - \mathbb{E}_{\mathbf{S}}(U_{t_0}^{\min}(A))| &< \eta/6 \\
|\mathbb{E}_{\mathbf{S}}(U_{t_0}(A + \varepsilon)) - \mathbb{E}_{\mathbf{S}}(T(A + \varepsilon))| &< \eta/6 \\
|\mathbb{E}_{\mathbf{S}}(U_{t_0}(A - \varepsilon)) - \mathbb{E}_{\mathbf{S}}(T(A - \varepsilon))| &< \eta/6 \\
|\mathbb{E}_{\mathbf{S}}(U_{t_0}(A)) - \mathbb{E}_{\mathbf{S}}(T(A))| &< \eta/6.
\end{aligned} \tag{58}$$

Finally, we just have to control  $2t_0(1 - P_{\mathbf{S}|\mathbf{S}^*}(\mathcal{C}_{t_0, \varepsilon}^{\mathbf{S}^*}))$ . Note that if  $\sup_{s \in \mathcal{S}_c} |\hat{\lambda}(s) - \lambda(s)| < \delta$  and  $S_1, \dots, S_{t_0} \in \mathcal{S}_c$ , then

$$\begin{aligned}
\sup_{t \leq t_0} |\tilde{R}_t - R_t| &= \sup_{t \leq t_0} \left| \max_{1 \leq k \leq t} \prod_{i=k}^t \hat{\lambda}(S_i) - \max_{1 \leq k \leq t} \prod_{i=k}^t \lambda(S_i) \right| \\
&\leq \sup_{t \leq t_0} \max_{1 \leq k \leq t} \left| \prod_{i=k}^t \hat{\lambda}(S_i) - \prod_{i=k}^t \lambda(S_i) \right| \\
&\leq \sup_{t \leq t_0} \max_{1 \leq k \leq t} \left( \max \{(u_\lambda + \delta)^{t-k} - u_\lambda^{t-k}, u_\lambda^{t-k} - (u_\lambda - \delta)^{t-k}\} \right) \\
&\leq \max \{(u_\lambda + \delta)^{t_0} - u_\lambda^{t_0}, u_\lambda^{t_0} - (u_\lambda - \delta)^{t_0}\},
\end{aligned} \tag{59}$$

since  $u_\lambda$  is the upper bound on  $\lambda$ . Then choose  $\delta_2 < \delta_1$  such that the right hand side is at most  $\varepsilon$ , so if  $\mathbf{S}^*$  is such that  $\sup_{s \in \mathcal{S}_c} |\hat{\lambda}(s) - \lambda(s)| < \delta_2$ , then  $P_{\mathbf{S}|\mathbf{S}^*}(\mathcal{C}_{t_0, \varepsilon}^{\mathbf{S}^*}) \geq (P_{\mathbf{S}}(S_i \in \mathcal{S}_c))^{t_0}$ . So choose  $c_2 < c_1$  such that

$$2t_0(1 - (P_{\mathbf{S}}(S_i \in \mathcal{S}_c))^{t_0}) < \eta/6. \quad (60)$$

Therefore,

$$P_{\mathbf{S}^*} \left( |\mathbb{E}_{\mathbf{S}|\mathbf{S}^*}(\tilde{T}(A)) - \mathbb{E}_{\mathbf{S}}(T(A))| < \eta \right) \geq P_{\mathbf{S}^*} \left( \sup_{s \in \mathcal{S}_{c_2}} |\hat{\lambda}(s) - \lambda(s)| < \delta_2 \right) P_{\mathbf{S}^*}(l_\lambda \leq \hat{\lambda} \ \forall s \in \text{supp}(S_i)) \rightarrow 1. \quad (61)$$

□

### A.3 Proof of Theorem 2

*Proof.* The proof is very similar to that of Theorem 1, using the same decomposition. The same arguments work to bound most of the decomposition, but we need to show two things: first, that we can control  $|\mathbb{E}_{\mathbf{S}|\mathbf{S}^*}(\tilde{T}_w(A)) - \mathbb{E}_{\mathbf{S}|\mathbf{S}^*}(\tilde{U}_{t_0, w}(A))|$ , and second that we can control  $P_{\mathbf{S}|\mathbf{S}^*}(\mathcal{C}_{t_0, \varepsilon}^{\mathbf{S}^*})$ .

To control  $|\mathbb{E}_{\mathbf{S}|\mathbf{S}^*}(\tilde{T}_w(A)) - \mathbb{E}_{\mathbf{S}|\mathbf{S}^*}(\tilde{U}_{t_0, w}(A))|$  we define  $\lambda_{\pi_0}^{\min}$ , similar to the  $\lambda_{\min}$  from the first proof. Suppose that  $|\hat{\pi}_\infty - \pi_\infty| < \xi$ , and let

$$\lambda_{\pi_0}^{\min}(s) = \begin{cases} \lambda_{\pi_0}(s) - \delta_1 & s \in \mathcal{S}_{c_1} \\ \min \left\{ \frac{a}{\pi_\infty + \xi}, \frac{1-b}{1-\pi_\infty + \xi} \right\} & s \notin \mathcal{S}_{c_1} \end{cases}. \quad (62)$$

Then if  $\sup_{\substack{s \in \mathcal{S}_{c_1} \\ \pi_0 \in \Pi_0}} |\hat{\lambda}_{\pi_0}(s) - \lambda_{\pi_0}(s)| < \delta_1$  we have  $\lambda_{\pi_0}^{\min}(s) \leq \hat{\lambda}_{\pi_0}(s)$  for all  $\pi_0$  and all  $s$ . The proof then proceeds as before.

For  $P_{\mathbf{S}|\mathbf{S}^*}(\mathcal{C}_{t_0, \varepsilon}^{\mathbf{S}^*})$ , we have that if  $\sup_{\substack{s \in \mathcal{S}_c \\ \pi_0 \in \Pi_0}} |\hat{\lambda}_{\pi_0}(s) - \lambda_{\pi_0}(s)| < \delta$  and  $S_1, \dots, S_{t_0} \in \mathcal{S}_c$ , then

$$\begin{aligned} \sup_{t \leq t_0} |\tilde{R}_t - R_t| &= \sup_{t \leq t_0} \left| \max_{\substack{t-m_\alpha \leq k \leq t \\ \pi_0 \in \Pi_0}} \int_{\Pi_0} \prod_{i=k}^t \hat{\lambda}_{\pi_0}(S_i) w(\pi_0) d\pi_0 - \max_{\substack{t-m_\alpha \leq k \leq t \\ \pi_0 \in \Pi_0}} \int_{\Pi_0} \prod_{i=k}^t \lambda_{\pi_0}(S_i) w(\pi_0) d\pi_0 \right| \\ &\leq \sup_{t \leq t_0} \max_{\substack{t-m_\alpha \leq k \leq t \\ \Pi_0}} \left| \int_{\Pi_0} \prod_{i=k}^t \hat{\lambda}_{\pi_0}(S_i) w(\pi_0) d\pi_0 - \int_{\Pi_0} \prod_{i=k}^t \lambda_{\pi_0}(S_i) w(\pi_0) d\pi_0 \right| \\ &\leq \sup_{t \leq t_0} \int_{\Pi_0} \left( \max_{\substack{t-m_\alpha \leq k \leq t \\ \Pi_0}} \left| \prod_{i=k}^t \hat{\lambda}_{\pi_0}(S_i) - \prod_{i=k}^t \lambda_{\pi_0}(S_i) \right| \right) w(\pi_0) d\pi_0 \\ &\leq \max \{ (M + \delta)^{m_\alpha} - M^{m_\alpha}, M^{m_\alpha} - (M - \delta)^{m_\alpha} \}. \end{aligned} \quad (63)$$

where  $M = \max \left\{ \frac{1}{\pi_\infty}, \frac{1}{1-\pi_\infty} \right\}$ . The proof then proceeds as before. □

### A.4 Proof of Corollary 1

We need to show that the conditions for Theorem III.2 in Unnikrishnan et al. (2011) hold, so we need to show that the  $g_\infty, g_0$  defined in (34) are a *joint stochastic bound* for  $(\mathcal{F}_\infty, \mathcal{F}_0)$ , where  $\mathcal{F}_\infty$  consists of all

distributions with densities

$$\pi_\infty f_\infty^1 + (1 - \pi_\infty) f_\infty^0 \quad \pi_\infty \in \Pi_\infty, \quad (64)$$

and  $\mathcal{F}_0$  consists of all distributions with densities

$$\pi_0 f_\infty^1 + (1 - \pi_0) f_\infty^0 \quad \pi_0 \in \Pi_0. \quad (65)$$

**Definition:** (see Unnikrishnan et al. (2011)) Let  $\mathcal{F}_\infty$  and  $\mathcal{F}_0$  be two classes of continuous distributions. Let  $Q_\infty \in \mathcal{F}_\infty$  and  $Q_0 \in \mathcal{F}_0$ , with associated densities  $q_\infty$  and  $q_0$ . Suppose that for all  $P_\infty \in \mathcal{F}_\infty$ ,  $P_0 \in \mathcal{F}_0$ , and all  $t$ ,

$$\begin{aligned} P_\infty \left( \frac{q_0(S)}{q_\infty(S)} > t \right) &\leq Q_\infty \left( \frac{q_0(S)}{q_\infty(S)} > t \right) \\ P_0 \left( \frac{q_0(S)}{q_\infty(S)} > t \right) &\geq Q_0 \left( \frac{q_0(S)}{q_\infty(S)} > t \right). \end{aligned} \quad (66)$$

Then we say  $(q_\infty, q_0)$  is a **joint stochastic bound** for  $(\mathcal{F}_\infty, \mathcal{F}_0)$ .

**Lemma 2.** Suppose that all distributions in  $\mathcal{F}_0$  are stochastically larger (smaller) than all distributions in  $\mathcal{F}_\infty$ , and  $Q_0$  is a stochastic lower (upper) bound on  $\mathcal{F}_0$  and  $Q_\infty$  is a stochastic upper (lower) bound on  $\mathcal{F}_\infty$ . If  $q_0/q_\infty$  is an increasing (decreasing) function, then  $(q_\infty, q_0)$  is a joint stochastic bound for  $(\mathcal{F}_\infty, \mathcal{F}_0)$ .

*Proof.* Suppose all distributions in  $\mathcal{F}_0$  are stochastically larger than all distributions in  $\mathcal{F}_\infty$ ,  $Q_0$  is a stochastic lower bound on  $\mathcal{F}_0$ ,  $Q_\infty$  is a stochastic upper bound on  $\mathcal{F}_\infty$ , and  $q_0/q_\infty$  is an increasing function (proof of the other case is similar). Then for any  $P_\infty \in \mathcal{F}_\infty$ ,  $P_0 \in \mathcal{F}_0$ ,

$$\begin{aligned} P_\infty \left( \frac{q_0(S)}{q_\infty(S)} > t \right) &= P_\infty \left( S > \left( \frac{q_0}{q_\infty} \right)^{-1}(t) \right) && \text{(increasing function)} \\ &\leq Q_\infty \left( S > \left( \frac{q_0}{q_\infty} \right)^{-1}(t) \right) && \text{(stochastic ordering)} \\ &= Q_\infty \left( \frac{q_0(S)}{q_\infty(S)} > t \right) \\ P_0 \left( \frac{q_0(S)}{q_\infty(S)} > t \right) &= P_0 \left( S > \left( \frac{q_0}{q_\infty} \right)^{-1}(t) \right) && \text{(increasing function)} \\ &\geq Q_0 \left( S > \left( \frac{q_0}{q_\infty} \right)^{-1}(t) \right) && \text{(stochastic ordering)} \\ &= Q_0 \left( \frac{q_0(S)}{q_\infty(S)} > t \right). \end{aligned} \quad (67)$$

□

Then it just remains to show that  $g_0/g_\infty$  is an increasing or decreasing function, and there is a stochastic ordering in the sets of distributions. A monotone likelihood ratio implies stochastic ordering, so it suffices to show that if  $s > s'$ ,

$$\text{sign} \left( \frac{\pi_0 f_\infty^1(s) + (1 - \pi_0) f_\infty^0(s)}{\pi_\infty f_\infty^1(s) + (1 - \pi_\infty) f_\infty^0(s)} - \frac{\pi_0 f_\infty^1(s') + (1 - \pi_0) f_\infty^0(s')}{\pi_\infty f_\infty^1(s') + (1 - \pi_\infty) f_\infty^0(s')} \right) = \text{sign}(\pi_0 - \pi_\infty). \quad (68)$$

If  $\pi_0 > \pi_\infty$ , then

$$\frac{f_\infty^1(s)}{f_\infty^0(s)} > \frac{f_\infty^1(s')}{f_\infty^0(s')} \implies \frac{\pi_0 f_\infty^1(s) + (1 - \pi_0) f_\infty^0(s)}{\pi_\infty f_\infty^1(s) + (1 - \pi_\infty) f_\infty^0(s)} > \frac{\pi_0 f_\infty^1(s') + (1 - \pi_0) f_\infty^0(s')}{\pi_\infty f_\infty^1(s') + (1 - \pi_\infty) f_\infty^0(s')}.$$
 (69)

Likewise, if  $\pi_0 < \pi_\infty$  then

$$\frac{f_\infty^1(s)}{f_\infty^0(s)} > \frac{f_\infty^1(s')}{f_\infty^0(s')} \implies \frac{\pi_0 f_\infty^1(s) + (1 - \pi_0) f_\infty^0(s)}{\pi_\infty f_\infty^1(s) + (1 - \pi_\infty) f_\infty^0(s)} < \frac{\pi_0 f_\infty^1(s') + (1 - \pi_0) f_\infty^0(s')}{\pi_\infty f_\infty^1(s') + (1 - \pi_\infty) f_\infty^0(s')}.$$
 (70)

Finally, under the assumption that  $P_\infty(Y = 1|s)$  is an increasing function of  $s$ , we have  $\frac{f_\infty^1(s)}{f_\infty^0(s)} > \frac{f_\infty^1(s')}{f_\infty^0(s')}$  since  $s > s'$ .

## A.5 Simulation Details

### A.5.1 Method Details

1. First, the baseline for detection is the **optimal CUSUM** procedure performed on the raw data  $X_1, X_2, \dots$ . When the true pre- and post-change distributions are known exactly, optimality of the CUSUM procedure means we can't do better than use the true likelihood ratio

$$\frac{\pi_0 f(X_i; \boldsymbol{\mu}_1, \boldsymbol{\Sigma}) + (1 - \pi_0) f(X_i; \boldsymbol{\mu}_0, \boldsymbol{\Sigma})}{\pi_\infty f(X_i; \boldsymbol{\mu}_1, \boldsymbol{\Sigma}) + (1 - \pi_\infty) f(X_i; \boldsymbol{\mu}_0, \boldsymbol{\Sigma})}.$$
 (71)

2. A relaxation of the assumptions for the optimal CUSUM procedure is that we know the parametric form of the pre- and post-change distributions, but must estimate the parameters. Let  $(X_1^*, Y_1^*), \dots, (X_{n_{est}}^*, Y_{n_{est}}^*) \sim \mathbb{P}_\infty$  be an estimation set, and let  $\widehat{\boldsymbol{\mu}}_0^*$ ,  $\widehat{\boldsymbol{\mu}}_1^*$ , and  $\widehat{\boldsymbol{\Sigma}}^*$  be the resulting parameter estimates. The likelihood ratio is

$$\frac{\pi_0 MVN(X_i; \widehat{\boldsymbol{\mu}}_1^*, \widehat{\boldsymbol{\Sigma}}^*) + (1 - \pi_0) MVN(X_i; \widehat{\boldsymbol{\mu}}_0^*, \widehat{\boldsymbol{\Sigma}}^*)}{\pi_\infty MVN(X_i; \widehat{\boldsymbol{\mu}}_1^*, \widehat{\boldsymbol{\Sigma}}^*) + (1 - \pi_\infty) MVN(X_i; \widehat{\boldsymbol{\mu}}_0^*, \widehat{\boldsymbol{\Sigma}}^*)}.$$
 (72)

For simulations, we will refer to this method as **GaussianEst**. It serves as essentially the best we can do, short of the optimal CUSUM procedure, when some estimation is involved in the distributions. Note that GaussianEst works with the raw  $X_i$  rather than the LDA scores  $S_i$ , so the parameter estimates  $\widehat{\boldsymbol{\mu}}_0$ ,  $\widehat{\boldsymbol{\mu}}_1$ , and  $\widehat{\boldsymbol{\Sigma}}$  from the training sample  $(X'_1, Y'_1), \dots, (X'_{n_{est}}, Y'_{n_{est}})$  could be used in the likelihood ratio instead. However, for consistency with other methods, we reserve the training sample for fitting the classifier, and the estimation sample for estimating pre- and post-change distributions.

3. If we don't know the parametric form of the  $X_i$  class distributions, we can instead work with the LDA scores and do density estimation on the LDA scores for each class. The resulting likelihood ratio is then

$$\frac{\pi_0 \widehat{f}_\infty^1(S_i) + (1 - \pi_0) \widehat{f}_\infty^0(S_i)}{\pi_\infty \widehat{f}_\infty^1(S_i) + (1 - \pi_\infty) \widehat{f}_\infty^0(S_i)}.$$
 (73)

This is the approach described in Lemma 1 and Theorem 1, which we will refer to as **KDE** for simulations. Theorem 1 shows that KDE should be asymptotically optimal.

For density estimation of scores in  $[0, 1]$ , we use the beta kernel density estimate from Chen (1999), as implemented in the R package `kdensity` (Moss and Tveten, 2019). The beta kernel density estimate provides a natural way to deal with scores on a bounded interval, particularly near the boundaries (see Figure 1). Density estimation is performed on the estimation sample  $\mathbf{S}^* = \mathcal{A}(X_1^*), \dots, \mathcal{A}(X_{n_{est}}^*)$ .

4. As discussed in Section 1.4, a wide variety of nonparametric procedures have been proposed when the pre- and post-change distributions are unknown. One approach is to replace the likelihood ratio  $\lambda(S_i)$  with some function  $g(S_i)$  that behaves similarly. In particular,  $g$  is chosen so that  $\mathbb{E}_\infty[\log g(S_i)] < 0$  and  $\mathbb{E}_0[\log g(S_i)] > 0$ . Here we implement the function described in Tartakovsky et al. (2012b), which is representative of similar functions, based on changes in means and/or variances, in the literature. The substitute  $g(S_i)$  for the likelihood ratio in CUSUM is

$$g(S_i) = \exp \left\{ \left( \frac{\hat{\mu}_{S,0}}{\hat{\sigma}_{S,0}^2} - \frac{\hat{\mu}_{S,\infty}}{\hat{\sigma}_{S,\infty}^2} \right) S_i + \left( \frac{1}{2\hat{\sigma}_{S,\infty}^2} - \frac{1}{2\hat{\sigma}_{S,0}^2} \right) S_i^2 + \log \left( \frac{\hat{\sigma}_{S,\infty}}{\hat{\sigma}_{S,0}} \right) + \left( \frac{\hat{\mu}_{S,\infty}^2}{2\hat{\sigma}_{S,\infty}^2} - \frac{\hat{\mu}_{S,0}^2}{2\hat{\sigma}_{S,0}^2} \right) \right\}, \quad (74)$$

where  $\mu_{S,j} = \mathbb{E}_j[S_i]$  and  $\sigma_{S,j}^2 = \text{Var}_j[S_i]$ , for  $j = 0, \infty$ . Estimates  $\hat{\mu}_{S,j}$  and  $\hat{\sigma}_{S,j}^2$  are computed from the estimation sample, with observations reweighted to estimate the post-change parameters. For example,

$$\begin{aligned} \hat{\mu}_{S,\infty} &= \frac{1}{n_{est}} \sum_{i=1}^{n_{est}} S_i^* \\ \hat{\mu}_{S,0} &= \pi_0 \left( \frac{1}{\sum_{i=1}^{n_{est}} \mathbb{1}\{Y_i^* = 1\}} \sum_{i=1}^{n_{est}} S_i^* \mathbb{1}\{Y_i^* = 1\} \right) + (1 - \pi_0) \left( \frac{1}{\sum_{i=1}^{n_{est}} \mathbb{1}\{Y_i^* = 0\}} \sum_{i=1}^{n_{est}} S_i^* \mathbb{1}\{Y_i^* = 0\} \right). \end{aligned} \quad (75)$$

The function  $g$  in (74) comes from the likelihood ratio of two Gaussians, but is recommended by Tartakovsky et al. (2012b) as a reasonable nonparametric procedure even when data are not normal. If  $g$  is close to  $\lambda$ , we would expect this procedure, which we refer to as **NPScore** in simulations, to perform well. However, in general there is no reason to expect  $g$  to be close to  $\lambda$ , so overall NPScore should do worse than KDE.

5. Another approach is to directly estimate the likelihood ratio, given data from  $\mathbb{P}_\infty$  and  $\mathbb{P}_0$ . This requires both pre- and post-change LDA scores. Given our estimation set  $\mathbf{S}^* = S_1^*, \dots, S_{n_{est}}^*$  of pre-change scores, we can create a set  $\tilde{S}_1^*, \dots, \tilde{S}_{n_{est}}^*$  of post-change scores by resampling with replacement from  $\mathbf{S}^*$ . In resampling, the probability of selecting  $S_i^*$  is  $\pi_0/\#\{Y_j^* = 1\}$  when  $Y_i^* = 1$ , and  $(1 - \pi_0)/\#\{Y_j^* = 0\}$  when  $Y_i^* = 0$ . One procedure for directly estimating the likelihood ratio is *unconstrained least-squares importance fitting* (**uLSIF**) (Kanamori et al., 2009), which models the likelihood ratio using kernel functions:

$$\hat{\lambda}(s) = \sum_{i=1}^{n_{est}} a_i K(s, \tilde{S}_i^*). \quad (76)$$

The coefficients  $a_i$  are estimated by minimizing a squared error loss, involving both  $S_1^*, \dots, S_{n_{est}}^*$  and  $\tilde{S}_1^*, \dots, \tilde{S}_{n_{est}}^*$  (Kanamori et al., 2009). For simulations, we used the implementation of uLSIF provided in the **R** package **densratio** (Makiyama, 2019).

If uLSIF does a good job at estimating the likelihood ratio, operating characteristics should be close to the optimal CUSUM procedure. However, we generally expect uLSIF to do worse than our KDE approach, because KDE uses the label-shift assumption in constructing the likelihood ratio.

6. While the nonparametric methods discussed so far use the CUSUM procedure with a substitute for the likelihood ratio, other nonparametric detection procedures have been proposed that avoid likelihood ratios and the CUSUM setup completely. For simulations, we consider the nearest-neighbors graph-based procedure discussed in Chen (2019); Chu and Chen (2018), specifically the weighted statistic described in Chu and Chen (2018). This statistic, implemented in the **R** package **gStream** (Chen and Chu, 2019), relies on a window size  $L$ , a number  $k$  of nearest neighbors, and a distance measure between observations. At time  $n$ , consider the window of the  $L$  most recent observations:  $X_{n-L+1}, \dots, X_n$ .

Compute the  $k$  nearest-neighbors graph for the full window. Now, each time  $t \in \{n - L + 1, \dots, n - 1\}$  divides the window into sub-windows  $X_{n-L+1}, \dots, X_t$  and  $X_{t+1}, \dots, X_n$ . If there has been no change, nearest-neighbor connections between sub-windows are as likely as connections within sub-windows. But if there has been a change, the structure of the graph looks different when comparing sub-windows. To turn this into a detection procedure, Chu and Chen (2018) summarize deviation from the expected structure in  $X_{n-L+1}, \dots, X_n$  with a detection statistic, and sound an alarm when the statistic exceeds a pre-determined threshold.

The advantage of this approach, which we will refer to as **kNN** in simulations, is that high-dimensional data can be analyzed and no assumptions on the pre- and post-change distributions are required. However, the absence of assumptions means the label shift structure cannot be leveraged, and so we expect our KDE approach to perform better. Note that the kNN procedure could be done with either raw data or LDA scores. We implement both in simulations, though we expect the results to be the same, since we shouldn't lose information by using LDA scores vs. the raw data.

### A.5.2 Summary of Main Simulations

Details of our main simulations are provided below. Simulations were implemented in **R** (R Core Team, 2020). To run simulations in parallel, we used the GNU parallel command-line tool (Tange, 2011).

---

#### Simulation Details

**Parameters:** Gaussian means  $\mu_0 = \mathbf{0}$  and  $\mu_1 \in \{[0.5, 0.5]^T, [1.5, 1.5]^T\}$  and covariance matrix  $\Sigma = \mathbf{I}$ ; pre- and post-change parameters  $\pi_\infty = 0.4$  and  $\pi_0 \in \{0.2, 0.4, 0.7\}$ ; training and estimation sample sizes  $n_{train}$  and  $n_{est}$ ; number of runs  $n_{runs}$  for Monte Carlo estimation of operating characteristics; number of different estimation samples  $n_{sims}$  for procedures with operating characteristics depending on the estimation sample; threshold  $A$  for CUSUM-based procedures; nearest-neighbors parameters  $L$  and  $k$

Draw LDA training data  $(X'_1, Y'_1), \dots, (X'_{n_{train}}, Y'_{n_{train}}) \sim \mathbb{P}_\infty$  as in (7). Use training data to fit the LDA classifier  $\mathcal{A}$ .

#### Optimal CUSUM:

```

for  $run \in \{1, \dots, n_{runs}\}$  do
  Draw  $(X_1, Y_1), (X_2, Y_2), \dots \sim \mathbb{P}_\infty$  as in (7)
  Perform CUSUM with likelihood ratio in (71), using threshold  $A$ 
  Record the stopping time  $T_{run,\infty}$ 

  Draw  $(X_1, Y_1), (X_2, Y_2), \dots \sim \mathbb{P}_0$  as in (7)
  Perform CUSUM with likelihood ratio in (71), using threshold  $A$ 
  Record the stopping time  $T_{run,0}$ 
end for
Return  $\frac{1}{n_{runs}} \sum_{run=1}^{n_{runs}} T_{run,\infty}$  (ARL) and  $\frac{1}{n_{runs}} \sum_{run=1}^{n_{runs}} T_{run,0}$  (detection delay)

```

#### GaussianEst:

```

for  $sim \in \{1, \dots, n_{sims}\}$  do
  Draw likelihood ratio estimation data  $(X_1^*, Y_1^*), \dots, (X_{n_{est}}^*, Y_{n_{est}}^*) \sim \mathbb{P}_\infty$  as in (7)
  Use estimation data  $(X_i^*, Y_i^*)$  to calculate  $\hat{\mu}_0^*, \hat{\mu}_1^*, \hat{\Sigma}^*$ 

  for  $run \in \{1, \dots, n_{runs}\}$  do
    Draw  $(X_1, Y_1), (X_2, Y_2), \dots \sim \mathbb{P}_\infty$  as in (7)
    Perform CUSUM with likelihood ratio in (72), using threshold  $A$ 
    Record the stopping time,  $T_{run,\infty}^{sim}$ 

```

Draw  $(X_1, Y_1), (X_2, Y_2), \dots \sim \mathbb{P}_0$  as in (7)  
 Perform CUSUM with likelihood ratio in (72), using threshold  $A$   
 Record the stopping time,  $T_{run,0}^{sim}$   
**end for**  
**end for**  
 For each  $sim$ , return  $\frac{1}{n_{runs}} \sum_{run=1}^{n_{runs}} T_{run,\infty}^{sim}$  (ARL) and  $\frac{1}{n_{runs}} \sum_{run=1}^{n_{runs}} T_{run,0}^{sim}$  (detection delay)

**KDE:**

**for**  $sim \in \{1, \dots, n_{sims}\}$  **do**  
 Draw likelihood ratio estimation data  $(X_1^*, Y_1^*), \dots, (X_{n_{est}}^*, Y_{n_{est}}^*) \sim \mathbb{P}_\infty$  as in (7)  
 Calculate LDA scores  $S_i^* = \mathcal{A}(X_i^*)$   
 Use estimation data  $\mathbf{S}^* = (S_1^*, \dots, S_{n_{est}}^*)$  to get density estimates  $\hat{f}_\infty^1, \hat{f}_\infty^0$   
  
**for**  $run \in \{1, \dots, n_{runs}\}$  **do**  
 Draw  $(X_1, Y_1), (X_2, Y_2), \dots \sim \mathbb{P}_\infty$  as in (7)  
 Calculate LDA scores  $S_i = \mathcal{A}(X_i)$   
 Perform CUSUM with likelihood ratio in (73), using threshold  $A$   
 Record the stopping time,  $T_{run,\infty}^{sim}$   
**end for**  
**end for**  
 For each  $sim$ , return  $\frac{1}{n_{runs}} \sum_{run=1}^{n_{runs}} T_{run,\infty}^{sim}$  (ARL) and  $\frac{1}{n_{runs}} \sum_{run=1}^{n_{runs}} T_{run,0}^{sim}$  (detection delay)

**NPScore:**

**for**  $sim \in \{1, \dots, n_{sims}\}$  **do**  
 Draw likelihood ratio estimation data  $(X_1^*, Y_1^*), \dots, (X_{n_{est}}^*, Y_{n_{est}}^*) \sim \mathbb{P}_\infty$  as in (7)  
 Calculate LDA scores  $S_i^* = \mathcal{A}(X_i^*)$   
 Use estimation data  $\mathbf{S}^* = (S_1^*, \dots, S_{n_{est}}^*)$  to get estimates  $\hat{\mu}_{S,0}, \hat{\mu}_{S,1}, \hat{\sigma}_{S,0}^2, \hat{\sigma}_{S,1}^2$   
  
**for**  $run \in \{1, \dots, n_{runs}\}$  **do**  
 Draw  $(X_1, Y_1), (X_2, Y_2), \dots \sim \mathbb{P}_\infty$  as in (7)  
 Calculate LDA scores  $S_i = \mathcal{A}(X_i)$   
 Perform CUSUM with likelihood ratio in (74), using threshold  $A$   
 Record the stopping time,  $T_{run,\infty}^{sim}$   
**end for**  
**end for**  
 For each  $sim$ , return  $\frac{1}{n_{runs}} \sum_{run=1}^{n_{runs}} T_{run,\infty}^{sim}$  (ARL) and  $\frac{1}{n_{runs}} \sum_{run=1}^{n_{runs}} T_{run,0}^{sim}$  (detection delay)

**uLSIF:**

**for**  $sim \in \{1, \dots, n_{sims}\}$  **do**  
 Draw likelihood ratio estimation data  $(X_1^*, Y_1^*), \dots, (X_{n_{est}}^*, Y_{n_{est}}^*) \sim \mathbb{P}_\infty$  as in (7)

Calculate LDA scores  $S_i^* = \mathcal{A}(X_i^*)$   
 Resample to get scores  $\tilde{S}_i^*$   
 Use  $S_1^*, \dots, S_{n_{est}}^*$  and  $\tilde{S}_1^*, \dots, \tilde{S}_{n_{est}}^*$  to estimate the likelihood ratio in (76)

```

for  $run \in \{1, \dots, n_{runs}\}$  do
    Draw  $(X_1, Y_1), (X_2, Y_2), \dots \sim \mathbb{P}_\infty$  as in (7)
    Calculate LDA scores  $S_i = \mathcal{A}(X_i)$ 
    Perform CUSUM with likelihood ratio in (76), using threshold  $A$ 
    Record the stopping time,  $T_{run, \infty}^{sim}$ 

    Draw  $(X_1, Y_1), (X_2, Y_2), \dots \sim \mathbb{P}_0$  as in (7)
    Calculate LDA scores  $S_i = \mathcal{A}(X_i)$ 
    Perform CUSUM with likelihood ratio in (76), using threshold  $A$ 
    Record the stopping time,  $T_{run, 0}^{sim}$ 
end for
end for
For each  $sim$ , return  $\frac{1}{n_{runs}} \sum_{run=1}^{n_{runs}} T_{run, \infty}^{sim}$  (ARL) and  $\frac{1}{n_{runs}} \sum_{run=1}^{n_{runs}} T_{run, 0}^{sim}$  (detection delay)

```

**kNN:**

```

for  $run \in \{1, \dots, n_{runs}\}$  do
    Draw  $(X_1, Y_1), (X_2, Y_2), \dots, (X_L, Y_L) \sim \mathbb{P}_\infty$  and  $(X_{L+1}, Y_{L+1}), \dots, (X_{2L}, Y_{2L}) \sim \mathbb{P}_0$  as in (7)
    Using  $X_1, \dots, X_L$  as historical data, begin kNN detection at time  $L + 1$ 
    Setting the kNN threshold to achieve a desired ARL, record the stopping time,  $T_{run, 0}^{\text{raw}}$ 

    Calculate the LDA scores  $S_i = \mathcal{A}(X_i)$ 
    Using  $S_1, \dots, S_L$  as historical data, begin kNN detection at time  $L + 1$ 
    Setting the kNN threshold to achieve a desired ARL, record the stopping time,  $T_{run, 0}^{\text{LDA}}$ 
end for
Return  $\frac{1}{n_{runs}} \sum_{run=1}^{n_{runs}} \min\{T_{run, 0} - L, L\}$  (lower bound on detection delay), and  $\sum_{run=1}^{n_{runs}} \mathbb{1}\{T_{run, 0} > 2L\}$ 

```

## A.6 Additional simulations

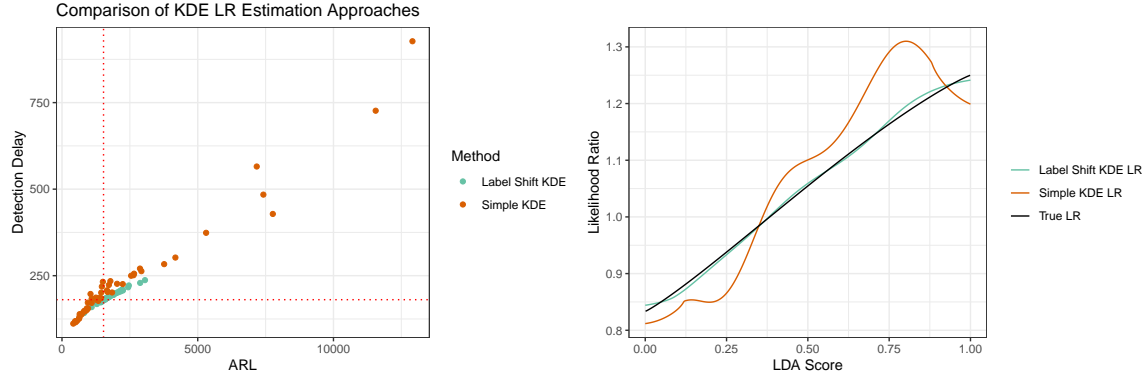


**Figure 7:** Our proposed KDE method (18) combines conditional score density estimates  $\tilde{f}_\infty^1$  and  $\tilde{f}_\infty^0$  using the label-shift assumption. If we didn't use the label-shift assumption, we could instead estimate the likelihood ratio by  $\hat{\lambda} = \tilde{f}_0/\tilde{f}_\infty$ , where  $\tilde{f}_\infty$  and  $\tilde{f}_0$  are density estimates of the marginal score densities  $f_\infty$  and  $f_0$ , computed from full pre- and post-change samples. This figure compares our label shift KDE with the simple KDE ratio that does not use the label-shift assumption. Left: (ARL, detection delay) pairs for 50 different estimation samples, with  $\mu_1 = [1.5, 1.5]^T$  and  $\pi_0 = 0.5$ . The dotted red lines show the optimal CUSUM detection delay and ARL at the threshold for which  $\text{ARL} \approx 1500$ . Right: The true LDA score-based likelihood ratio function is shown as a black curve. Example likelihood ratio functions, from one estimation sample, are compared for the label shift KDE and simple KDE.

Parameters		CPM Detection Delay when ARL = 1000 (proportion of changes not detected)
$\mu_1$	$\pi_0$	
$[0.5, 0.5]^T$	0.2	$\geq 446$ (0.24)
	0.5	$\geq 489$ (0.32)
	0.7	$\geq 386$ (0.11)
$[1.5, 1.5]^T$	0.2	$\geq 291$ (0.01)
	0.5	$\geq 422$ (0.18)
	0.7	221 (0)

**Table 4:** Sequential detection of label shift was also considered in Ackerman et al. (2020), in which the authors propose using Cramer–von-Mises tests in a nonparametric sequential detection procedure, using the R changepoint detection package `cpm` (Ross, 2015). For comparison with our results, as presented in Table 1, we estimated average detection delay of this CPM method for each of our simulation settings. Because the `cpm` package only supports a fixed list of ARL options, we chose ARL = 1000, which was closest to the ARL = 1500 used in our main simulations. For computational purposes, we fixed the number of post-change observations at 1000. For some sequences no change was observed before time 1000, so our observed average detection delay is a lower bound, and we report the fraction of runs in which no change was observed.